Dickkopf-1 promotes hematopoietic regeneration via direct and niche-mediated mechanisms

Heather A Himburg[1,7], Phuong L Doan[2,7], Mamle Quarmyne[1,3], Xiao Yan[1,3], Joshua Sasine[1], Liman Zhao[1], Grace V Hancock[4], Jenny Kan[1], Katherine A Pohl[1], Evelyn Tran[1], Nelson J Chao[2], Jeffrey R Harris[2] & John P Chute[1,5,6]

The role of osteolineage cells in regulating hematopoietic stem cell (HSC) regeneration following myelosuppression is not well understood. Here we show that deletion of the pro-apoptotic genes *Bak* and *Bax* in osterix (Osx, also known as Sp7 transcription factor 7)-expressing cells in mice promotes HSC regeneration and hematopoietic radioprotection following total body irradiation. These mice showed increased bone marrow (BM) levels of the protein dickkopf-1 (Dkk1), which was produced in Osx-expressing BM cells. Treatment of irradiated HSCs with Dkk1 *in vitro* increased the recovery of both long-term repopulating HSCs and progenitor cells, and systemic administration of Dkk1 to irradiated mice increased hematopoietic recovery and improved survival. Conversely, inducible deletion of one allele of *Dkk1* in Osx-expressing cells in adult mice inhibited the recovery of BM stem and progenitor cells and of complete blood counts following irradiation. Dkk1 promoted hematopoietic regeneration via both direct effects on HSCs, in which treatment with Dkk1 decreased the levels of mitochondrial reactive oxygen species and suppressed senescence, and indirect effects on BM endothelial cells, in which treatment with Dkk1 induced epidermal growth factor (EGF) secretion. Accordingly, blockade of the EGF receptor partially abrogated Dkk1-mediated hematopoietic recovery. These data identify Dkk1 as a regulator of hematopoietic regeneration and demonstrate paracrine cross-talk between BM osteolineage cells and endothelial cells in regulating hematopoietic reconstitution following injury.

Perivascular stromal cells and vascular endothelial cells (ECs) regulate HSC maintenance in the BM of mice[1–3]. Deletion of nestin-expressing mesenchymal stromal cells (MSCs) has also been shown to decrease HSC content in the BM, which is associated with HSC mobilization[4]. Leptin receptor (Lepr)- and paired related homeobox 1 (Prx1)-expressing perivascular cells and nestin-expressing stromal cells have been postulated to represent overlapping perivascular populations which regulate HSC maintenance *in vivo*[5,6]. Recently, maintenance of quiescent, long-term repopulating HSCs was suggested to be dependent on chondroitin sulfate proteoglycan 4 (Cspg4+ or NG2+) pericytes localized to the arteriolar vascular niche, which are distinct from Lepr-expressing peri-sinusoidal cells[7]. These studies have confirmed the importance of perivascular cells and vascular ECs in regulating HSC maintenance.

Expansion of the BM osteoblast population has been shown to amplify the HSC pool *in vivo*[8,9], and ganciclovir-inducible depletion of BM osteoblasts decreases phenotypic hematopoietic stem and progenitor cell content[10]. However, deletion of the genes encoding stem cell factor (SCF), the chemokine CXCL12 or N-cadherin in BM osteoblasts does not have effects on HSC content during homeostasis[1–3,11]. Sp7 (Osx) is a transcription factor expressed by mesenchymal progenitor cells, which have been shown via lineage tracing to be osteolineage-restricted in the adult mouse[6,12,13]. In the fetal BM,

Osx-expressing cells contribute to nascent bone tissues and transient stromal cells, whereas perinatally, Osx-expressing cells contribute to long-lived MSCs and osteolineage cells[6,13]. Notably, deletion of *Dicer1*, which encodes an RNaseIII endonuclease, in Osx-expressing cells promotes myelodysplasia in mice, suggesting that aberrant function of Osx-expressing cells may contribute to the development of hematologic malignancy[14]. Deletion of *CXCL12* from Osx-expressing cells was also shown to deplete B lymphoid progenitors in homeostasis, but no effect on HSC function was observed[3].

Although genetic studies have provided insight into the function of BM niche cells in regulating hematopoiesis during homeostasis, important questions remain regarding the contributions of niche cells during stress or injury, as well as the effects of injury on niche-mediated regulation of HSCs. We and others have recently demonstrated the essential role of BM ECs in regulating HSC regeneration following myelotoxicity[15–17], and we identified two BM EC-derived paracrine factors, pleiotrophin (PTN) and EGF, as regulators of HSC regeneration *in vivo*[18,19]. However, the functions of BM mesenchymal and osteolineage cells in regulating HSC regeneration remain less well understood. Here we directly tested the function of Osx-expressing BM cells in regulating hematopoietic regeneration following myelosuppression and discovered that Osx-expressing BM cells promote hematopoietic regeneration via secretion of Dkk1.

[1]Division of Hematology and Oncology, Department of Medicine, University of California, Los Angeles (UCLA), Los Angeles, California, USA. [2]Division of Hematologic Malignancies and Cellular Therapy, Duke University, Durham, North Carolina, USA. [3]Department of Pharmacology and Cancer Biology, Duke University, Durham, North Carolina, USA. [4]Department of Cell and Developmental Biology, University of California, Los Angeles, Los Angeles, California, USA. [5]Broad Center for Regenerative Medicine and Stem Cell Research, University of California, Los Angeles, Los Angeles, California, USA. [6]Jonsson Comprehensive Cancer Center, University of California, Los Angeles, Los Angeles, California, USA. [7]These authors contributed equally to this work. Correspondence should be addressed to J.P.C. (jchute@mednet.ucla.edu).

RESULTS

Deletion of *Bak* and *Bax* in Osx-expressing cells radioprotects the hematopoietic system

To test whether radioprotection of these cells would alter the hematopoietic response to irradiation, we used Cre-*loxP* technology to delete *loxP*-flanked (floxed; FL) genes encoding the pro-apoptotic factors Bak and Bax in Osx-expressing cells (from *Sp7–Cre;Bak1$^{-/-}$;Bax$^{FL/-}$* mice, hereafter referred to as *Osx–Cre;Bak1$^{-/-}$;Bax$^{FL/-}$* mice)[15,20]. To determine the proportion of Osx-labeled cells that expressed Osx in 8-week-old mice, we used Sp7–Cherry (hereafter referred to as Osx–Cherry) reporter mice, because these mice have a stronger reporter signal than mice with a GFP reporter driven by *Osx–Cre*. In 8-week-old Osx–Cherry reporter mice, approximately 60% of Cherry-labeled BM cells expressed Osx, as measured by flow cytometry, whereas in 5-d-old mice, 83% of Cherry-labeled BM cells expressed Osx (**Fig. 1a**). These results indicate that a subset of Osx-labeled BM cells lose Osx protein expression between birth and adulthood. Adult *Osx–Cre;Bak1$^{-/-}$;Bax$^{FL/-}$* mice showed no baseline differences in the frequency of Osx$^+$ BM cells, BM trabecular bone content, complete blood counts, HSC content or repopulating HSC function, as compared to those in *Osx–Cre;Bak1$^{-/-}$;Bax$^{FL/+}$* control mice, which retain one wild-type allele of *Bax* (**Supplementary Fig. 1a–g**). Next we irradiated both strains of mice with 500 cGy total body irradiation (TBI) to assess the response of Osx-expressing BM cells and of hematopoietic stem and progenitor cells to injury. *Osx–Cre;Bak1$^{-/-}$;Bax$^{FL/-}$* mice maintained Osx$^+$ BM cells at day 3 after irradiation as compared to *Osx–Cre;Bak1$^{-/-}$;Bax$^{FL/+}$* mice, which showed depletion of this population (**Fig. 1b** and **Supplementary Fig. 1h**). As compared to *Osx–Cre;Bak1$^{-/-}$;Bax$^{FL/+}$* mice at day 7 after TBI, *Osx–Cre;Bak1$^{-/-}$;Bax$^{FL/-}$* mice displayed increased BM cellularity, increased numbers of c-kit$^+$Sca-1$^+$lineage$^-$ (KSL) stem–progenitors, SLAM$^+$KSL HSCs, colony-forming cells (CFCs), and peripheral blood (PB) white blood cells (WBCs), neutrophils and lymphocytes (**Fig. 1c–f**). In competitive transplantation experiments, congenic Bl6.SJL mice transplanted with BM cells from *Osx–Cre;Bak1$^{-/-}$;Bax$^{FL/-}$* mice showed a significant increase in multilineage hematopoietic cell reconstitution in both primary and secondary transplanted mice, as compared to mice that were transplanted with BM from *Osx–Cre;Bak1$^{-/-}$;Bax$^{FL/+}$* mice (**Fig. 1g,h**). Taken together, these data suggest that the hematopoietic response to radiation injury is regulated by Osx-expressing BM cells and that deletion of the intrinsic pathway of apoptosis in these cells promotes radioprotection of the hematopoietic system.

Dkk1 is differentially expressed by Osx$^+$ BM cells

Because *Osx–Cre;Bak1$^{-/-}$;Bax$^{FL/-}$* mice showed enhanced hematopoietic recovery following TBI, we hypothesized that Osx-expressing BM cells might produce factors that promote hematopoietic regeneration. Analysis of BM supernatants from *Osx–Cre;Bak1$^{-/-}$;Bax$^{FL/-}$* mice revealed enrichment for several candidate proteins as compared to *Osx–Cre;Bak1$^{-/-}$;Bax$^{FL/+}$* mice (**Supplementary Fig. 2a**). Among these candidates, we focused on Dkk1, a Wnt inhibitor, because Dkk1 was previously shown to be expressed and secreted by osteolineage cells under the control of osterix[21], although it has no established role in regulating hematopoietic regeneration. Furthermore, in preliminary screening experiments we found that Dkk1 promoted CFC recovery from BM KSL cells that were irradiated with 300 cGy *in vitro*, whereas two other candidates, tissue inhibitor of metalloproteinase 2 (Timp2) and the chemokine Ccl20 (also known as MIP-3a), had no effect (data not shown). ELISA confirmed that *Osx–Cre;Bak1$^{-/-}$;Bax$^{FL/-}$* mice contained significantly higher levels of Dkk1 protein

in the BM than *Osx–Cre;Bak1$^{-/-}$;Bax$^{FL/+}$* mice (**Fig. 1i**). Expression of *Dkk1* mRNA was also significantly increased in BM osteolineage cells from *Osx–Cre;Bak1$^{-/-}$;Bax$^{FL/-}$* mice, as compared to that in *Osx–Cre;Bak1$^{-/-}$;Bax$^{FL/+}$* mice; in both mouse strains, nearly all of the detectable Dkk1 protein was found in Osx$^+$ BM cells, as assessed by flow cytometry (**Fig. 1j** and **Supplementary Fig. 2b**). Moreover, we found that Osx$^+$ BM cells expressed significantly more Dkk1 than BM ECs in C57BL/6 mice, both at steady state and following TBI (**Fig. 1k**). These results indicate that Osx$^+$ BM cells are the primary source of Dkk1 in both *Osx–Cre;Bak1$^{-/-}$;Bax$^{FL/-}$* and wild-type mice.

Dkk1 treatment accelerates hematopoietic regeneration *in vitro* and *in vivo*

We next sought to evaluate whether Dkk1 regulates hematopoietic regeneration following irradiation. First, we assessed the effect of Dkk1 on the function of non-irradiated HSCs *in vitro* and *in vivo*. Treatment of non-irradiated BM KSL cells with 500 ng/ml Dkk1 in medium supplemented with thrombopoietin (TPO), SCF and Flt-3 ligand had no effect on total cell expansion, KSL expansion or CFC content, as compared to cells treated with medium alone (**Supplementary Fig. 3a,b**). However, systemic treatment of C57BL/6 mice with 10 µg Dkk1 subcutaneously every other day for 4 weeks caused a significant increase in the numbers of BM KSL cells, BM c-kit$^+$lin$^-$ cells and BM CFCs, as well as in the PB neutrophil frequency, compared to saline-treated mice (**Supplementary Fig. 3c–e**). These data suggest that during homeostasis, Dkk1 promotes the *in vivo* expansion of the myeloid progenitor cell pool.

To evaluate the function of Dkk1 in regulating hematopoietic regeneration following irradiation, we irradiated BM KSL cells with 300 cGy and cultured them in cytokine-containing medium with or without 500 ng/ml Dkk1. Dkk1 treatment significantly increased the recovery of CFCs at day 7 of culture, as compared to treatment with cytokines alone (**Fig. 2a**). Furthermore, mice that had been competitively transplanted with the progeny of irradiated, Dkk1-treated KSL cells showed a significant increase in multilineage engraftment of donor CD45.2$^+$ cells over the course of 16 weeks after transplantation (**Fig. 2b**). These results suggest that Dkk1 directly promotes the regeneration of HSCs capable of primary competitive repopulation following irradiation.

Because Dkk1 promotes the regeneration of irradiated hematopoietic stem and progenitor cells (HSPCs) *in vitro*, we next tested whether systemic administration of Dkk1 could accelerate hematopoietic regeneration *in vivo* following TBI. Adult C57BL/6 mice were irradiated with 800 cGy TBI and treated subcutaneously with 10 µg Dkk1 or saline every other day for 21 d, beginning at day 1 after TBI. Systemic administration of Dkk1 caused a greater than eightfold increase in Dkk1 levels in the BM of C57BL/6 mice within 1 h, as compared to untreated mice (**Fig. 2c**). Dkk1 treatment increased the recovery of WBCs, neutrophil counts, platelets and BM cell counts at day 21 as compared to saline-treated mice (**Fig. 2d,e**). Furthermore, the numbers of BM KSL cells and CFCs were significantly increased in Dkk1-treated mice as compared to those in saline-treated controls (**Fig. 2f,g**). Notably, following 800 cGy TBI, only 4 of 15 (27%) C57BL/6 mice that had been treated with saline survived to day 30, as compared to 13 of 14 mice (93%) that had been treated with Dkk1, a nearly 350% increase in survival in response to Dkk1 treatment ($P = 0.0004$) (**Fig. 2h**).

We also evaluated whether Dkk1 treatment could affect long-term hematopoiesis in mice following radiation exposure. Adult C57BL/6 mice were irradiated with 600 cGy TBI, treated with 10 µg Dkk1 every other day for 21 d and evaluated at 12 weeks after irradiation. As compared

to saline-treated controls, Dkk1-treated mice showed no differences in complete blood counts and BM cell counts, percentages of SLAM+KSL or KSL cells, or frequencies of BM myeloid cells, B cells or T cells (**Supplementary Fig. 4a–c**). However, at 12 weeks following 600-cGy irradiation, saline-treated mice had substantially reduced numbers of BM CFCs as compared to irradiated, Dkk1-treated mice (**Fig. 2i**). These data suggest that TBI causes a long-term decline in myeloid progenitor

cell function and that short-term treatment with Dkk1 abrogates radiation-induced damage to this progenitor cell population.

Inhibition of Dkk1 abrogates hematopoietic regeneration following TBI

Because systemic administration of Dkk1 augments hematopoietic regeneration and survival of mice following TBI, we next tested
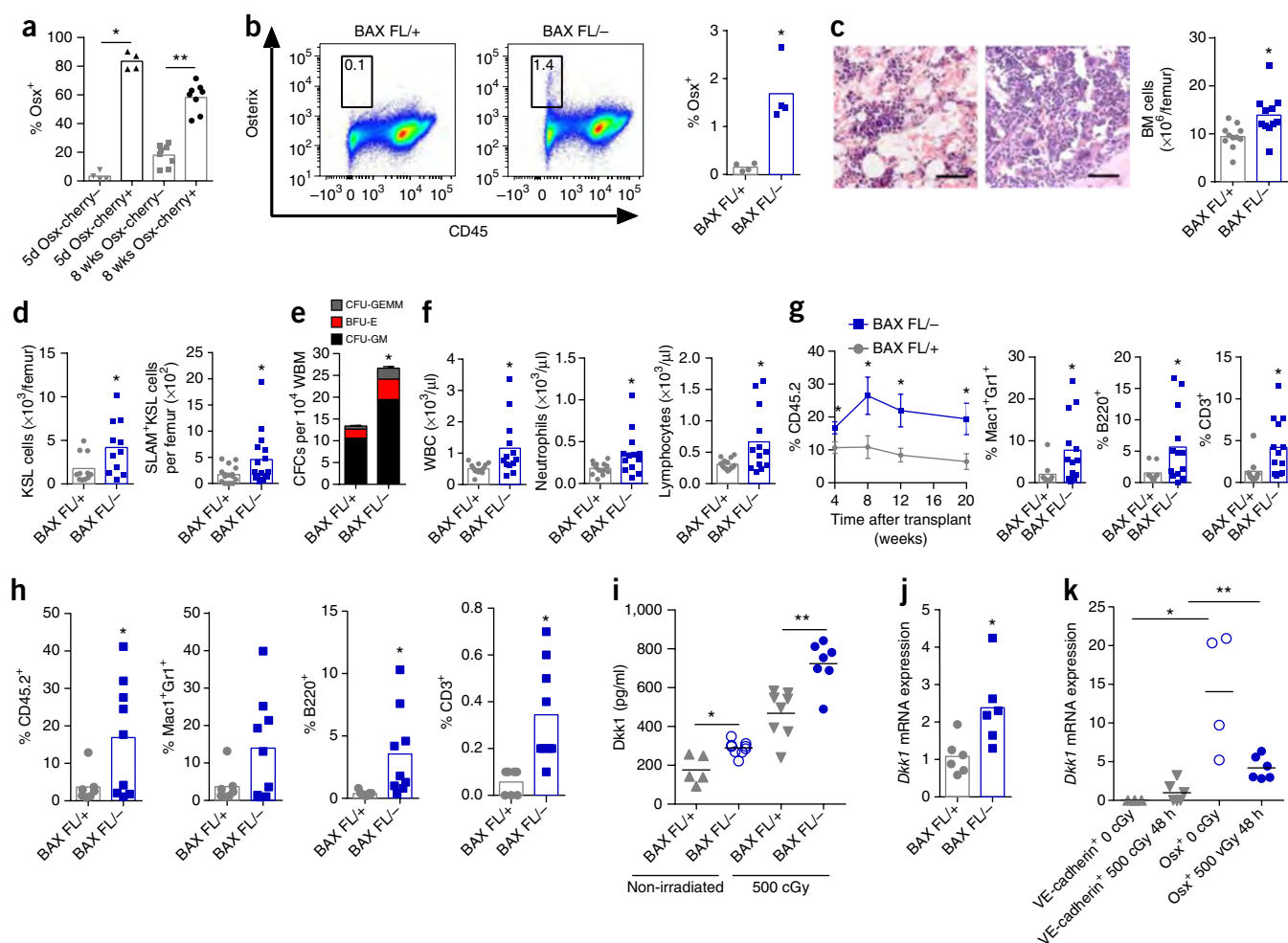
Figure 1 Deletion of *Bak* and *Bax* in Osx+ BM cells radioprotects hematopoietic stem and progenitor cells. (**a**) Mean percentages of Osx+ cells, as measured by flow cytometry, within Osx-labeled BM cells (Osx–cherry+) and Osx-unlabeled cells (Osx–cherry−) from 5-d-old ($n = 4$ mice/group) and 8-week-old ($n = 8$ mice/group) Osx–Cherry reporter mice. *$P < 0.001$, **$P < 0.001$. (**b**) Left, representative FACS plots showing the percentage of Osx+ cells in CD45− BM cells in *Osx–Cre;Bak1−/−;BaxFL/+* (BAX FL/+) and *Osx–Cre;Bak1−/−;BaxFL/−* (BAX FL/−) mice at day +3 following 500 cGy TBI. Right, the mean percentage of Osx+CD45− BM cells ($n = 4$ mice/group). *$P = 0.004$. (**c**) Representative images of H&E-stained femurs from BAX FL/+ (left) and BAX FL/− (middle) mice at day +7 following 500 cGy TBI (40×; scale bars, 100 μm) and scatter plot of BM cell counts for mice in each group ($n = 11$ mice/group) (right). Horizontal lines represent means. *$P = 0.009$. (**d**) Mean numbers of BM KSL cells (*$P = 0.03$) (left) and SLAM+KSL cells (*$P = 0.04$) (right) in BAX FL/+ and BAX FL/− mice at day +7 following 500 cGy TBI ($n = 11$ mice/group). (**e**) Mean numbers of BM CFCs at day +7 ($n = 21$ assays/group). WBM, whole bone marrow; CFU-GM, colony-forming unit–granulocyte monocyte; BFU-E, burst-forming unit–erythroid; CFU-GEMM, colony-forming unit–mix. *$P < 0.0001$. (**f**) Mean PB WBC (*$P = 0.01$) (left), neutrophil (*$P = 0.02$) (middle) and lymphocyte (*$P = 0.02$) (right) counts at day +7 (FL/+, $n = 14$ mice; FL/−, $n = 13$ mice). (**g**) Donor (CD45.2+) cell engraftment over time in recipient CD45.1+ mice that were transplanted with 1×10^6 BM cells from BAX FL/+ or BAX FL/− mice and 1×10^5 competing, non-irradiated host BM cells. *$P = 0.03$, *$P = 0.03$, *$P = 0.02$ and *$P = 0.04$ for 4, 8, 12 and 20 weeks, respectively. Myeloid (Mac1/Gr1; *$P = 0.04$), B cell (B220; *$P = 0.04$) and T cell (CD3; *$P = 0.03$) engraftment levels at 20 weeks are shown (4, 8 and 12 weeks: FL/+, $n = 14$ mice; FL/−, $n = 15$ mice; 20 weeks: FL/+, $n = 9$ mice; FL/−, $n = 13$ mice). (**h**) Mean levels of donor CD45.2+ cell and lineage engraftment in secondary recipient CD45.1+ mice at 20 weeks following competitive transplantation with BM cells from primary mice (FL/+, $n = 7$ mice; FL/−, $n = 9$ mice). CD45.2+, *$P = 0.04$; B220+, *$P = 0.03$; CD3+, *$P = 0.004$. (**i**) Mean Dkk1 levels in the BM of non-irradiated or irradiated (500 cGy) BAX FL/+ and BAX FL/- mice. *$P < 0.001$ and **$P < 0.001$ (NI FL/+, $n = 5$ mice; NI FL/-, $n = 9$ mice; IRR FL/+, $n = 8$ mice; IRR FL/-, $n = 7$ mice). (**j**) Mean expression of Dkk1 in BM osteolineage cells in BAX FL/− mice relative to that in BAX FL/+ mice ($n = 6$ mice/group). *$P = 0.02$. (**k**) *Dkk1* expression in VE-cadherin+ BM ECs and Osx+ BM cells in mice before (0 cGy; VE-cadherin+, $n = 3$ mice; Osx+, $n = 4$ mice) and 48 h after 500 cGy TBI ($n = 6$ mice/group). *Dkk1* expression levels in all groups were normalized to that in VE-cadherin+ BM ECs at 48 h. *$P = 0.03$ and **$P = 0.003$. Throughout, P values were derived by using a two-tailed Student's *t*-test.
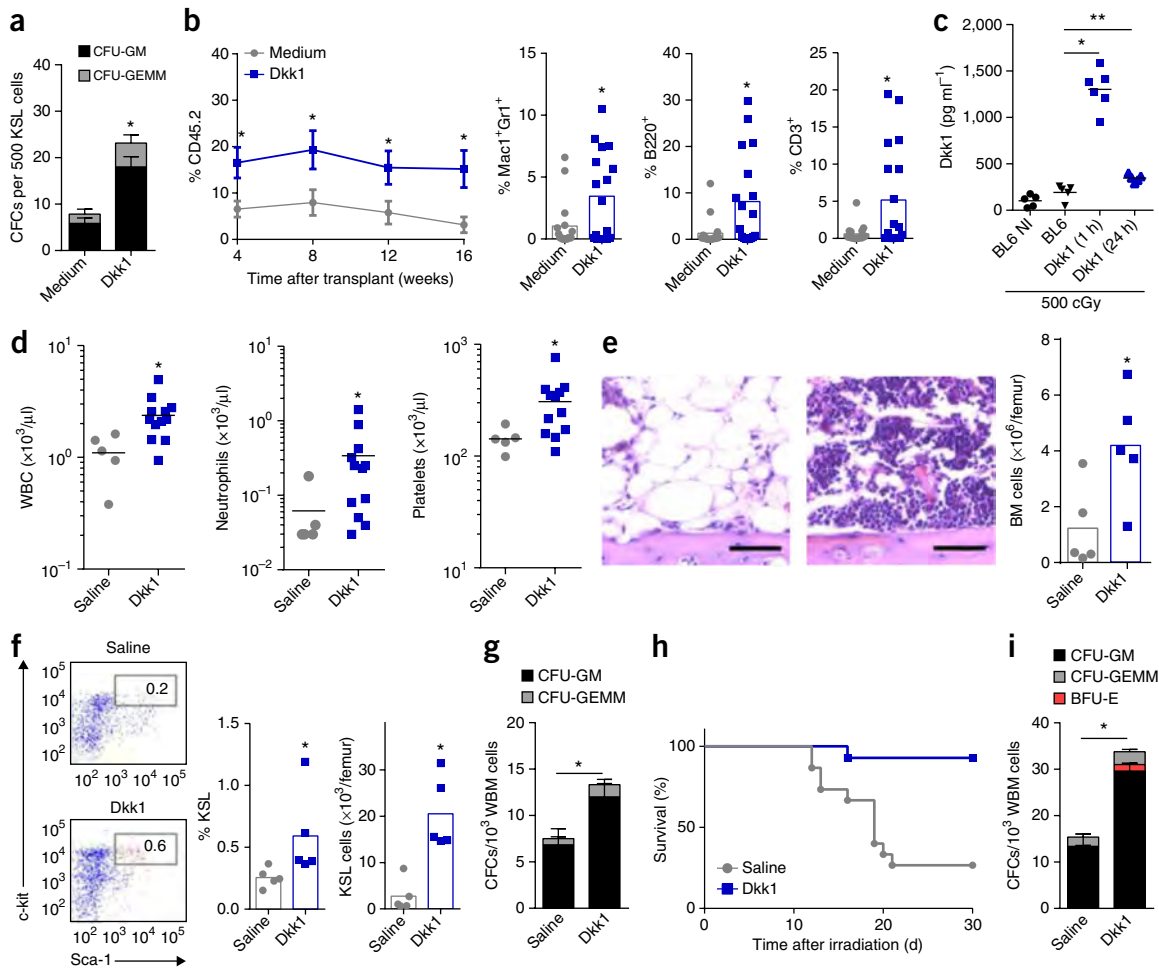
Figure 2 Dkk1 promotes hematopoietic regeneration *in vitro* and *in vivo*. (**a**) Mean numbers of CFCs recovered from 7-d cultures of irradiated (300 cGy) BM KSL cells that were treated with TPO, SCF and Flt-3 ligand (TSF)-containing medium (medium), with or without 500 ng/ml Dkk1 ($n = 3$ assays/group). *$P = 0.003$. (**b**) Left, mean percentage of donor CD45.2$^+$ cell engraftment levels in recipient CD45.1$^+$ mice over time following competitive transplantation with the progeny of 1×10^4 irradiated (300 cGy) BM KSL cells that were cultured with or without 500 ng/ml Dkk1 for 7 d. *$P = 0.01$, *$P = 0.03$, *$P = 0.03$, *$P = 0.01$ for 4, 8, 12 and 16 weeks, respectively. Right, mean percentages of donor myeloid (*$P = 0.02$), B cell (*$P = 0.01$) and T cell (*$P = 0.01$) engraftment at 16 weeks in recipient mice ($n = 17$ mice/group). (**c**) Dkk1 concentrations in the BM of mice at baseline, following 500 cGy treatment, and at 1 h and 24 h following administration of 10 µg Dkk1 administration (BL6 non-irradiated (NI), $n = 5$ mice; BL6, $n = 5$ mice; Dkk1 (1 h), $n = 6$ mice; Dkk1 (24 h), $n = 5$ mice). *$P < 0.001$, **$P < 0.001$. (**d**) Scatter plots of PB WBCs (left), neutrophils (middle) and platelet (right) counts at day +21 from mice irradiated with 800 cGy and then treated with saline or Dkk1 (saline, $n = 5$ mice; Dkk1, $n = 12$ mice). *$P = 0.008$, *$P = 0.02$, *$P = 0.01$; by Mann–Whitney U test. (**e**) Left, representative images of H&E-stained femurs from saline-treated (left) and Dkk1-treated (middle) mice at day +21 following treatment with 800 cGy (40×; scale bars, 100 µm). Right, mean BM cell counts ($n = 5$ mice/group). *$P = 0.02$. (**f**) Left, representative FACS plots showing the percentage of BM KSL cells in saline-treated and Dkk1-treated mice at day +21 following treatment with 800 cGy TBI. Middle and right, the mean percentage of KSL cells (*$P = 0.02$) (middle) and KSL cell numbers (*$P = 0.008$) (right) ($n = 5$ mice/group). P values determined by Mann–Whitney U test. (**g**) Mean numbers of BM CFCs at day +21 following treatment with 800 cGy TBI ($n = 6$ assays/group). *$P = 0.04$. (**h**) Survival of saline-treated (4/15) or Dkk1-treated (13/14) mice following treatment with 800 cGy TBI (27% versus 93%; $P = 0.0004$ by log-rank test). (**i**) Mean numbers of CFCs in C57BL/6 mice at 12 weeks after 600 cGy TBI and treatment with 10 µg Dkk1 or saline, subcutaneously, every other day through day +21 ($n = 5$ assays/group). *$P = 0. 001$. Throughout, unless otherwise noted, P values were derived by using a two-tailed Student's t-test.

whether endogenous Dkk1 is necessary for normal hematopoietic regeneration following TBI. We irradiated adult C57BL/6 mice with a sublethal TBI dose of 500 cGy and then administered 100 µg of a blocking Dkk1-specific antibody or an IgG control antibody every other day for 14 d. Anti-Dkk1 treatment significantly lowered Dkk1 levels in the BM at 24 h after treatment (**Supplementary Fig. 5a**). At day 10 following irradiation, mice that were treated with anti-Dkk1 had a significant decrease in BM cell counts and in the numbers of PB WBCs, neutrophils, lymphocytes, KSL cells and CFCs, as compared to those in irradiated, IgG-treated mice (**Fig. 3a–c** and **Supplementary Fig. 5b**). Furthermore, treatment with anti-Dkk1 caused a significant

decrease in the 30-d survival of irradiated mice (6 of 12 alive, 50%) as compared to irradiated controls (12 of 12, 100%; $P = 0.006$) (**Fig. 3d**). Taken together, these results suggest that endogenous Dkk1 plays an important role in regulating hematopoietic regeneration and survival following myelosuppression.

Deletion of Dkk1 in Osx-expressing BM cells inhibits hematopoietic regeneration

We next tested whether deletion of a single allele of Dkk1 in Osx-labeled cells (*Osx–Cre;Dkk1$^{FL/+}$* mice) would affect the hematopoietic response to TBI as compared to *Dkk1$^{+/+}$* mice. 8-week-old *Osx–Cre;Dkk1$^{FL/+}$*
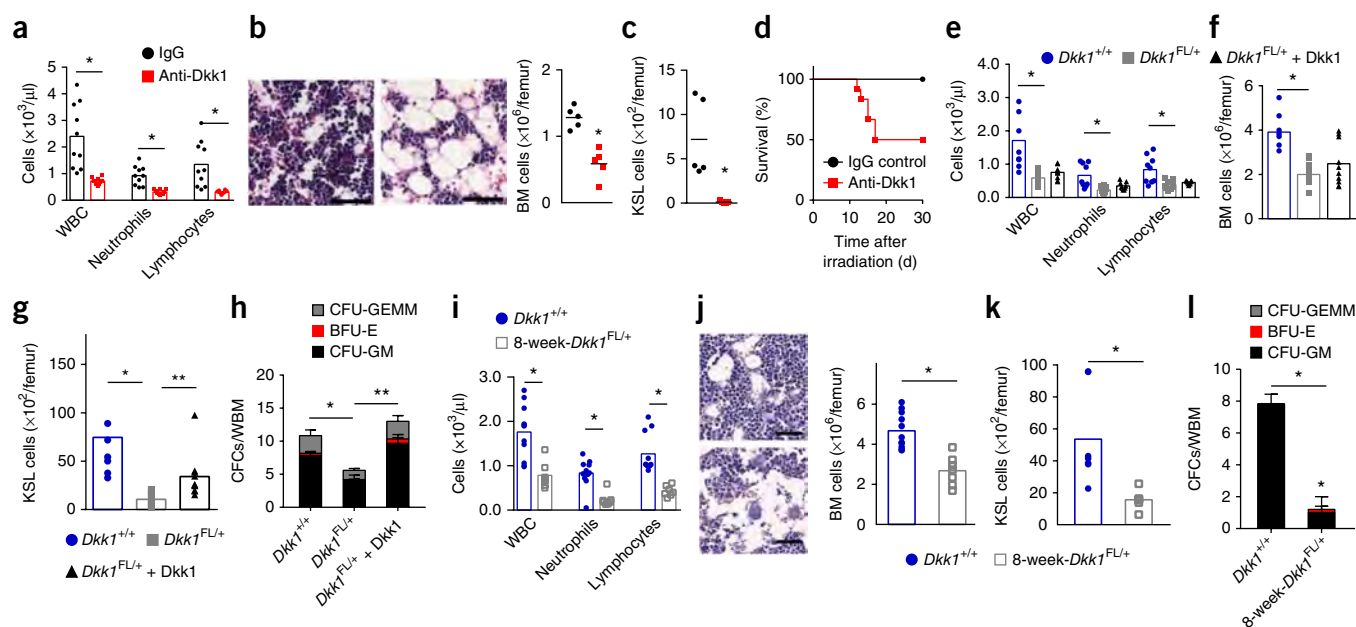
Figure 3 Inhibition or deficiency of Dkk1 in Osx-expressing BM cells suppresses hematopoietic regeneration. (**a**) PB WBCs, neutrophils and lymphocytes in mice treated with anti-Dkk1 or control IgG at day +10 following 500 cGy TBI. *$P = 0.0004$, *$P < 0.0001$, *$P = 0.002$, respectively ($n = 10$ mice/group). (**b**) Left, representative images of H&E-stained femurs stained with IgG (top) or anti-Dkk1 (bottom) at day +10 (40×; scale bars, 50 μm). Right, BM cell counts at day +10 ($n = 5$ mice/group). *$P < 0.001$. (**c**) Mean KSL cell numbers at day +10 ($n = 5$ mice/group). *$P = 0.007$. (**d**) Survival analysis of mice irradiated with 750 cGy TBI and treated with anti-Dkk1 or IgG ($n = 12$ mice/group). $P = 0.006$. (**e**) The hematopoietic profiles (PB WBCs (*$P < 0.001$), neutrophils (*$P = 0.001$) and lymphocytes (*$P = 0.007$)) of *Osx–Cre;Dkk1$^{FL/+}$* (*Dkk1$^{FL/+}$*) and *Osx–Cre;Dkk1$^{+/+}$* (*Dkk1$^{+/+}$*) mice at day 10 after irradiation with 500 cGy TBI and of irradiated *Dkk1$^{FL/+}$* mice that were treated every other day with Dkk1 through day +10 (*Dkk1$^{FL/+}$* + Dkk1) and evaluated at day +10 (*Dkk1$^{+/+}$*, $n = 9$ mice; *Dkk1$^{FL/+}$*, $n = 10$ mice; *Dkk1$^{FL/+}$* + Dkk1, $n = 10$ mice). (**f**) BM cell counts at day +10 (*Dkk1$^{+/+}$*, $n = 9$ mice; *Dkk1$^{FL/+}$*, $n = 10$ mice; *Dkk1$^{FL/+}$* + Dkk1, $n = 10$ mice). *$P < 0.001$. (**g**) BM KSL cell numbers at day +10 (*Dkk1$^{+/+}$*, $n = 7$ mice; *Dkk1$^{FL/+}$*, $n = 10$ mice; *Dkk1$^{FL/+}$* + Dkk1, $n = 10$ mice). *$P = 0.002$, **$P = 0.03$. (**h**) Mean numbers of BM CFCs at day +10 (*Dkk1$^{+/+}$*, $n = 6$ assays; *Dkk1$^{FL/+}$*, $n = 6$ assays; *Dkk1$^{FL/+}$* + Dkk1, $n = 3$ assays). *$P = 0.008$, **$P = 0.005$. (**i**) Mean concentrations of PB WBCs (*$P = 0.001$), neutrophils (*$P < 0.001$) and lymphocytes (*$P < 0.001$) in *Osx–Cre;Dkk1$^{+/+}$* mice (*Dkk1$^{+/+}$*) and 8-week-*Osx–Cre;Dkk1$^{FL/+}$* mice (8-week-*Dkk1$^{FL/+}$*) at day +10 following 500 cGy TBI (*Dkk1$^{+/+}$*, $n = 11$ mice; 8-week-*Dkk1$^{FL/+}$*, $n = 7$ mice). (**j**) Left, representative images of H&E-stained femurs from *Dkk1$^{+/+}$* (top) and 8-week-*Dkk1$^{FL/+}$* (bottom) mice at day +10 (40×; scale bars, 50 μm). Right, mean BM cell counts per femur (*Dkk1$^{+/+}$*, $n = 11$ mice; 8-week-*Dkk1$^{FL/+}$*, $n = 7$ mice). *$P < 0.001$. (**k**) Mean BM KSL cells at day +10 (*Dkk1$^{+/+}$*, $n = 7$ mice; 8-week-*Dkk1$^{FL/+}$*, $n = 6$ mice). *$P = 0.01$. (**l**) Mean BM CFCs at day +10 (*Dkk1$^{+/+}$*, $n = 6$ assays; 8-week-*Dkk1$^{FL/+}$*, $n = 3$ assays). *$P = 0.005$. Throughout, P values were derived by using a two-tailed Student's t-test.

mice showed no significant differences in hematologic profile or BM stem and progenitor cell content at baseline compared to that in *Dkk1$^{+/+}$* mice (**Supplementary Fig. 6a–d**). However, at day 10 following 500-cGy TBI, *Osx–Cre;Dkk1$^{FL/+}$* mice showed a significant decrease in the numbers of WBCs, neutrophils and lymphocytes, as compared to those in *Dkk1$^{+/+}$* mice (**Fig. 3e**). BM cell counts and the number of BM KSL cells, CFCs, BM myeloid cells, T cells and B cells were also decreased significantly in *Osx–Cre;Dkk1$^{FL/+}$* mice as compared to those in *Dkk1$^{+/+}$* mice (**Fig. 3f–h** and **Supplementary Fig. 6e**). These data suggest that endogenous Dkk1, produced by Osx-labeled BM cells, has a necessary role in regulating the hematopoietic response to irradiation.

Next we treated 500-cGy-irradiated *Osx–Cre;Dkk1$^{FL/+}$* mice with 10 μg of Dkk1 every other day for 10 d to determine whether Dkk1 treatment could rescue the hematopoietic phenotype of these mice. Although Dkk1 treatment did not alter the complete blood counts or BM cell counts in *Osx–Cre;Dkk1$^{FL/+}$* mice at day 10 after TBI, this treatment did significantly increase the numbers of BM KSL cells and BM CFCs, as compared to those in untreated mice (**Fig. 3e–h**). These results provide evidence that *Dkk1* deletion is responsible for the BM stem and progenitor cell abnormalities observed early after radiation injury in *Osx–Cre;Dkk1$^{FL/+}$* mice.

Our initial analysis of *Osx–Cre;Dkk1$^{FL/+}$* mice, in which the Cre protein was expressed from inception, did not allow for discrimination between the effects of *Dkk1* deletion in Osx-expressing osteoprogenitors and those in Osx-expressing long-lived MSCs in the BM, which can persist into adulthood[6]. In *Osx–Cre;Dkk1$^{FL/+}$* mice, expression of a tetracycline transactivator under the regulation of the osterix (*Sp7*) promoter controls the expression of a tetracycline response element (TRE)-controlled Cre fusion protein[22], such that doxycycline (Dox) administration prevents Cre-mediated recombination in Osx-expressing cells (Dox-Off). To study the effects of *Dkk1* deletion starting at 8 weeks of age and older, we treated *Osx–Cre;Dkk1$^{FL/+}$* mice with Dox from inception to 8 weeks of age (hereafter referred to as 8-week-*Osx–Cre;Dkk1$^{FL/+}$* mice). Irradiation of 8-week-*Osx–Cre;Dkk1$^{FL/+}$* mice with 500 cGy TBI at 10 weeks of age caused a significant decrease in the numbers of PB WBCs, neutrophils and lymphocytes, as well as in BM cell counts and in the numbers of BM KSL cells and BM CFCs at day 10 following TBI, as compared to those in *Osx–Cre;Dkk1$^{+/+}$* mice (**Fig. 3i–l**). The enhanced hematopoietic toxicity following TBI that was observed in 8-week-*Osx–Cre;Dkk1$^{FL/+}$* mice was comparable to that observed in *Osx–Cre;Dkk1$^{FL/+}$* mice bearing a *Dkk1* deletion from inception, suggesting that BM osteoprogenitor cells are the primary source of Dkk1 in regulating hematopoietic regeneration.

Dkk1 suppresses reactive oxygen species generation and p38-mediated senescence in irradiated HSCs

Ionizing radiation can cause hematopoietic injury via generation of reactive oxygen species (ROS) and induction of HSC senescence[23]. At 24 h following 300-cGy irradiation of cells *in vitro*, the levels of mitochondrial ROS increased substantially in BM CD34⁻KSL cells,

KSL cells and lineage-negative (lin⁻) cells (**Fig. 4a** and **Supplementary Fig. 7a**). Treatment with 500 ng/ml Dkk1 suppressed radiation-induced mitochondrial ROS generation in each cell population (**Fig. 4a** and **Supplementary Fig. 7a**). *In vivo*, systemic Dkk1 treatment of C57BL/6 mice irradiated with 500 cGy TBI resulted in a significant decrease in the levels of mitochondrial ROS in BM CD34⁻KSL cells
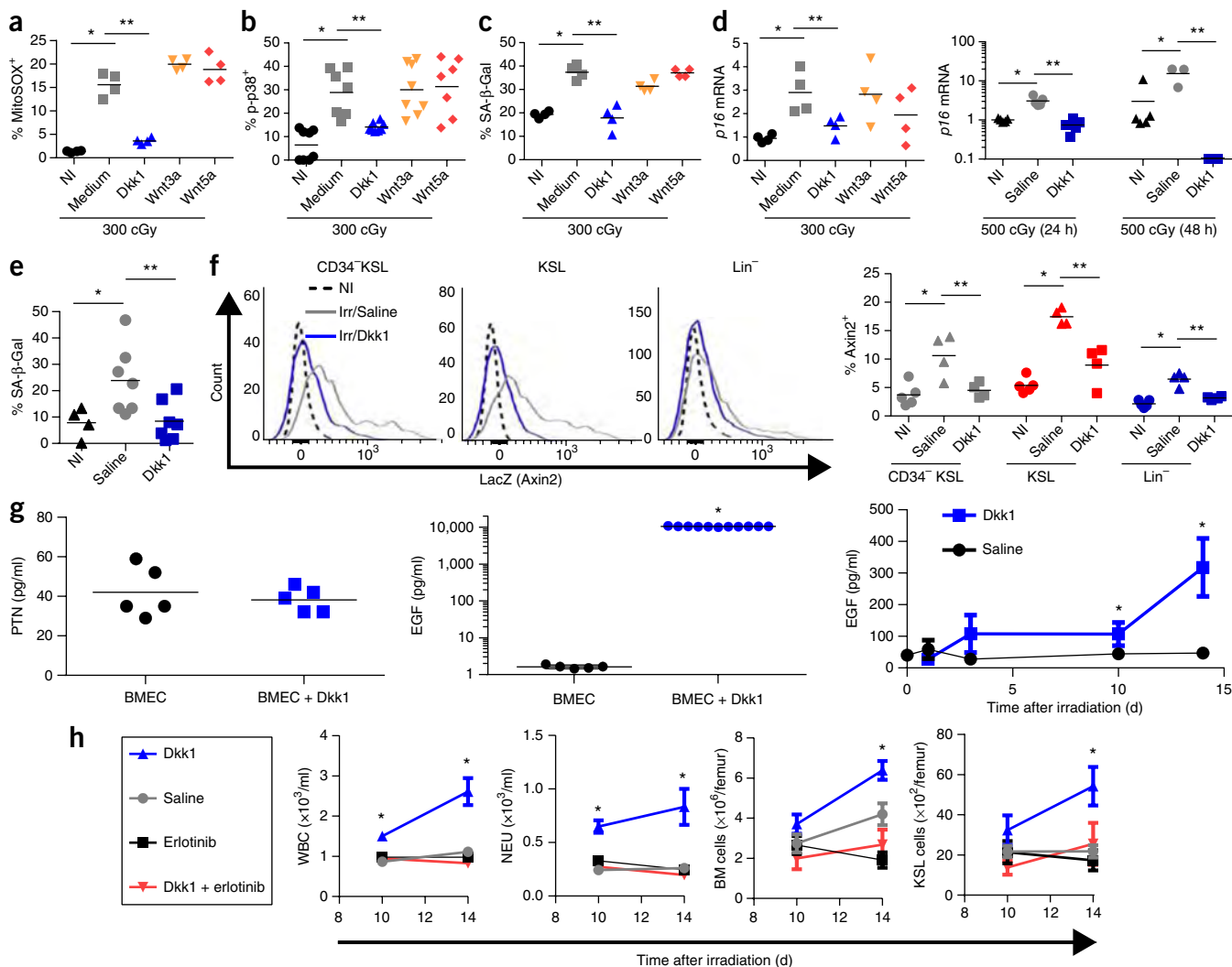
Figure 4 Dkk1 suppresses HSC senescence following irradiation and induces EGF secretion by BM ECs. (**a**) The percentage of MitoSOX⁺ cells in non-irradiated CD34⁻ KSL cells (NI) and at 24 h after 300 cGy TBI without treatment (medium) or with treatment with 500 ng/ml Dkk1, 100 ng/ml Wnt3a or 200 ng/ml Wnt5a; treatment was initiated 15 min before irradiation ($n = 4$ cell cultures/group). Medium included TPO, SCF and Flt-3 ligand. *$P < 0.001$, **$P < 0.001$. (**b**) The percentage of phospho-p38-positve cells in CD34⁻ KSL cells at 24 h after 300 cGy irradiation (NI, $n = 8$ cultures; medium, $n = 7$ cultures; Dkk1, $n = 8$ cultures; Wnt3a, $n = 8$ cultures; Wnt5a, $n = 7$ cultures). *$P < 0.001$, **$P < 0.001$. (**c**) The percentage of SA–β-gal⁺ CD34⁻ KSL cells at 24 h after 300 cGy irradiation ($n = 4$ cultures/group). *$P < 0.001$, **$P < 0.001$. (**d**) Left, *p16* gene expression in BM CD34⁻ KSL cells at 24 h after 300 cGy irradiation in the indicated treatment groups. *$P = 0.005$, **$P = 0.02$ ($n = 4$ cultures/group). Right, *p16* expression in BM KSL cells at 24 and 48 h after 500 cGy TBI in mice treated without (saline) or with 10 µg Dkk1 ($n = 4$ cultures/group). 24 h, *$P < 0.001$, **$P < 0.001$; 48 h, *$P = 0.02$, **$P = 0.02$. (**e**) Mean percentages of SA–β-gal⁺ BM KSL cells in non-irradiated mice and in mice at 12 weeks following 600 cGy TBI and treated with saline or 10 µg Dkk1 every other day through day +21 (NI, $n = 4$ mice; saline, $n = 7$ mice; Dkk1, $n = 7$ mice). *$P = 0.04$, **$P = 0.02$. (**f**) Left, representative histograms of Axin2–LacZ⁺ cells within BM CD34⁻ KSL cells, KSL cells and lin⁻ cells in mice at 24 h after 500 cGy TBI in the treatment groups shown. Right, the mean percentage of Axin2⁺ cells in each cell population at 24 h following 500 cGy TBI with and without Dkk1 treatment ($n = 4$ mice/group). CD34⁻ KSL cells, *$P = 0.009$, **$P = 0.01$; KSL cells, *$P < 0.001$, **$P = 0.004$; lin⁻ cells, *$P < 0.001$, **$P = 0.002$. (**g**) Left, mean levels of PTN in cultures of BM ECs ($n = 5$ cultures/group). Middle, mean levels of EGF in BM ECs in response to 500 ng/nl Dkk1 treatment (*$P < 0.001$; BMEC, $n = 5$ cultures; BMEC + Dkk1, $n = 10$ cultures). Right, mean levels of EGF in C57BL/6 mice over time following 500 cGy TBI and treatment with saline or 10 µg Dkk1 every other day through day +14 ($n = 5$ mice/group) (day +10, *$P = 0.03$; day +14, *$P = 0.02$). (**h**) Mean values for PB WBCs, neutrophils, BM cell counts and BM KSL cells at days +10 and +14 following 500 cGy TBI and treatment with saline or 10 µg Dkk1, with and without 10 µg/g erlotinib ($n = 5$ mice/group). WBCs: day +10, *$P < 0.001$; day +14, *$P = 0.002$; neutrophils: day +10, *$P < 0.001$; day +14, *$P = 0.01$; BM cell counts: day +14, *$P = 0.02$; BM KSL cells: day +14, *$P = 0.01$. Throughout, *P* values were derived by using a two-tailed Student's *t*-test.

at 24 h after irradiation (**Supplementary Fig. 7b**). *In vitro* treatment with Wnt3a (a canonical Wnt agonist) or Wnt5a (a noncanonical Wnt ligand) did not significantly alter mitochondrial ROS levels in irradiated CD34⁻KSL cells, KSL cells or lin⁻ cells beyond the effects observed with radiation alone (**Fig. 4a** and **Supplementary Fig. 7a**). Consistent with its effects on decreasing ROS levels in irradiated HSCs, Dkk1 treatment of BM CD34⁻KSL cells increased CFC recovery *in vitro* (**Supplementary Fig. 7c**). However, in the presence of a ROS scavenger, *N*-acetylcysteine (NAC), Dkk1 treatment did not increase CFC recovery from irradiated KSL cells, suggesting that Dkk1-mediated hematopoietic regeneration is dependent, at least in part, on suppression of ROS (**Supplementary Fig. 7c**). Elevated ROS levels drive activation of p38 mitogen-activated protein kinase (MAPK), which mediates a cytokine release phenomenon associated with senescence[23,24]. Irradiation significantly increased p38 phosphorylation in BM CD34⁻KSL cells at 24 h after exposure, and this increase was significantly attenuated by Dkk1 treatment (**Fig. 4b**). Of note, Dkk1 treatment had more modest effects in reducing p38 phosphorylation in irradiated BM KSL and lin⁻ cells (**Supplementary Fig. 7e**). Dkk1 treatment also significantly reduced senescence-associated β-galactosidase (SA–β-gal) levels in irradiated BM CD34⁻KSL cells, KSL cells and lin⁻ cells (**Fig. 4c** and **Supplementary Fig. 7f**). In contrast, treatment with Wnt3a or Wnt5a had no significant effects on either p38 phosphorylation or SA–β-gal levels in irradiated BM CD34⁻KSL cells (**Fig. 4b,c**). In keeping with its observed effects on SA–β-gal levels, Dkk1 suppressed radiation-induced expression of the p16-encoding isoform of cyclin-dependent kinase inhibitor 2a (*Cdkn2a*; hereafter referred to as *p16*) in BM CD34⁻KSL cells *in vitro* and attenuated *p16* expression in BM KSL cells in mice that were irradiated with 500 cGy (**Fig. 4d**). Dkk1 treatment also suppressed HSC apoptosis in irradiated BM KSL cells, as measured by caspase-3–caspase-7 activation (**Supplementary Fig. 7g**).

Next we extended our analysis of the effects of Dkk1 on radiation-induced senescence of BM HSC and progenitor cell populations by evaluating the long-term effects of systemic Dkk1 treatment on irradiated mice. At 12 weeks following 600 cGy TBI, C57BL/6 mice showed an increased frequency of SA–β-gal⁺ KSL cells, consistent with the idea that senescent BM stem and progenitor cells persist following radiation injury (**Fig. 4e**). This observation is in accord with a recent study that demonstrated that TBI induces persistent senescence of HSCs and premature aging of the hematopoietic system[25]. Notably, mice that were treated with Dkk1 every other day through day 21 following TBI showed a significantly lower percentage of SA–β-gal⁺ KSL cells at 12 weeks, as compared to untreated, irradiated mice (**Fig. 4e**). Coupled with our observation that Dkk1 treatment led to an increase in BM CFCs at 12 weeks following irradiation (**Fig. 2i**), these data suggest that short-term treatment with Dkk1 promotes longer-term recovery of hematopoietic progenitor cells following radiation injury.

Dkk1 inhibits Wnt pathway activation in irradiated HSCs
Dkk1 is a member of the Dkk family of secreted proteins that can inhibit Wnt signaling via binding and sequestration of the Wnt co-receptors, LRP5 and LRP6[26]. Using Axin2–LacZ reporter mice as previously described[27,28], we evaluated Wnt pathway activation in BM HSC and progenitor cell subsets in response to irradiation and Dkk1 treatment. Exposure of mice to 500 cGy TBI increased Wnt signaling in BM CD34⁻KSL cells, KSL cells and lin⁻ cells at 24 h after exposure (**Fig. 4f**). This activation of Wnt signaling was suppressed by Dkk1 treatment in these cell populations at 24 h after irradiation, as measured by the percentage of Axin2⁺ cells and the mean fluorescence

intensity (MFI) of the Axin2–lacZ signal (**Fig. 4f** and **Supplementary Fig. 8a**). Of note, Wnt pathway activation in response to irradiation seemed to be stronger in the BM CD34⁻KSL cells and the KSL cells as compared to that in BM lin⁻ cells (**Fig. 4f**). As assessed by the percentage of Axin2⁺ cells, Dkk1-mediated suppression of Wnt signaling was comparable across the three cell populations, although MFI analysis suggested that Dkk1 had the strongest suppressive effect in BM KSL cells (**Supplementary Fig. 8a**). *Axin2* mRNA levels increased concordantly in BM KSL cells in mice at 24 h after 500 cGy TBI, and this increase in *Axin2* mRNA was abrogated by Dkk1 treatment (**Supplementary Fig. 8b**).

To determine the functional relevance of Wnt inhibition to Dkk1-mediated hematopoietic regeneration, we used a viral Cre–based approach to delete *Ctnnb1*, the gene encoding β-catenin, in BM KSL cells from *Ctnnb1*^FL/FL^ mice (**Supplementary Fig. 9a**)[29]. At 96 h following 300 cGy irradiation *in vitro*, Dkk1 treatment decreased ROS generation in *Ctnnb1*^+/+^ BM KSL cells but not in *Ctnnb1*^−/−^ KSL cells (**Supplementary Fig. 9b**). Similarly, Dkk1 treatment increased CFC recovery at 96 h after irradiation from *Ctnnb1*^+/+^ KSL cells but not from *Ctnnb1*^−/−^ KSL cells (**Supplementary Fig. 9c**). These data suggest that Wnt pathway inhibition contributes, at least in part, to the early effects of Dkk1 on ROS generation and hematopoietic progenitor recovery.

Dkk1 promotes hematopoietic regeneration via induction of EGF secretion by BM ECs
Next we tested the possibility that there might be cross-talk between Dkk1 and pleiotrophin (PTN) or EGF, two vascular-niche-derived proteins that we have previously shown to be HSC regenerative factors[16,18,19]. We first tested whether treatment of primary BM osteolineage cells (Osx⁺osteocalcin⁺ cells cultured from femur bone explants) with PTN or EGF could induce Dkk1 secretion. However, this was not observed in 7-d culture; indeed, EGF treatment significantly reduced Dkk1 secretion (**Supplementary Fig. 10**). Next we asked whether Dkk1 could induce the secretion of these paracrine factors by primary BM ECs, as BM ECs are known to regulate HSC regeneration[15,17,30,31]. Although Dkk1 treatment did not induce the secretion of PTN by primary BM ECs, it induced a greater than 5,000-fold increase in EGF levels after 7 d, as compared to that in untreated BM ECs (**Fig. 4g**). Systemic administration of Dkk1 to mice irradiated with 500 cGy caused a marked increase in EGF levels in the BM at days 10 and 14 following radiation (**Fig. 4g**). To test the functional relevance of Dkk1-mediated induction of EGF secretion to hematopoietic regeneration, we orally administered 10 µg per g body weight of erlotinib, an EGF receptor antagonist, daily for 10 d to 500-cGy-irradiated, Dkk1-treated mice. Erlotinib treatment abrogated Dkk1-mediated recovery of PB WBCs, neutrophils, BM cell counts and BM KSL cells at day 10 and day 14, as compared to that in mice treated with Dkk1 alone (**Fig. 4h**). These results suggest that, in addition to its direct effects on hematopoietic cells, Dkk1 promotes hematopoietic regeneration via induction of EGF secretion by BM ECs.

DISCUSSION
The functions of BM osteolineage cells and MSCs in regulating HSC regeneration are incompletely understood[32,33]. Here we demonstrate that deletion of a single allele of *Dkk1* in Osx-expressing BM cells abrogates hematopoietic regeneration following irradiation. Inducible deletion of *Dkk1* in Osx-expressing cells in >8-week-old mice caused a comparable defect in hematopoietic regeneration in response to TBI as observed in mice bearing deletion of *Dkk1* from inception

in Osx-expressing cells. These data suggest that BM osteoprogenitor cells, rather than long-lived MSCs, are the primary source of Dkk1 that regulates hematopoietic regeneration in adult mice.

In gain-of-function studies, systemic Dkk1 treatment accelerated hematopoietic regeneration and improved survival following lethal dose TBI. This marked improvement in survival may have been related to the augmented recovery of myeloid progenitor cells, which have been shown to mediate survival following lethal dose TBI[34]. Dkk1 treatment also directly promoted the regeneration of HSCs with competitive repopulating capacity following irradiation *in vitro*. In a prior study of Dkk1 transgenic mice by Fleming *et al.*, overexpression of Dkk1 at steady state was associated with an increased frequency of HSCs capable of primary competitive repopulation, coupled with a deficiency in HSCs capable of serial transplantation[35]. In the current study, we examined the effects of Dkk1 treatment or *Dkk1* deletion on the hematopoietic regenerative response to myelotoxic injury, whereas Fleming *et al.* described the hematopoietic effects of Dkk1 overexpression during homeostasis[35]. It is possible that Dkk1-mediated signaling has distinct effects on HSCs in the setting of stress versus homeostasis, as has been demonstrated for Notch signaling[36]. Furthermore, we found that Dkk1 treatment induces BM ECs to secrete EGF, a regenerative factor for HSCs[19], an effect that likely also contributes to the differences in the results of our study as compared to the prior study by Fleming *et al.*[35].

Ionizing radiation causes the generation of ROS in HSCs, and ROS accumulation contributes to radiation-induced HSC apoptosis and senescence[23,37,38]. ROS are also deleterious to short- and long-term HSC function and HSC self-renewal capacity[39,40]. ROS promote HSC senescence via activation of p38 MAPK and p16[23,24]. Conversely, FoxO proteins are essential for downregulating ROS levels in HSCs, and transfer of ROS via gap junctions containing gap junction protein alpha 1 (Gja1; also known as connexin-43) to BM stromal cells can mitigate ROS-mediated HSC senescence[39,40]. Notably, ROS generation occurs during BM or cord blood collection in ambient air, and this was recently shown to be highly damaging to HSC yield and function[41]. Furthermore, high-dose irradiation has been shown to markedly increase pO_2 concentrations in HSC niches via BM vascular disruption[42]. These findings underscore the therapeutic importance of suppressing ROS after myelosuppressive injury and may explain, in part, the potency of Dkk1 administration in promoting the survival of lethally irradiated mice.

Canonical Wnt signaling has been shown to regulate the fate of HSCs, myeloid progenitors and T cell subsets in a dosage-dependent manner[26–28,43]. Using Axin2–lacZ reporter mice, we observed that TBI rapidly induced Wnt pathway activation in HSCs and progenitor cells and that systemic treatment with Dkk1 suppressed this response. Dkk1 also suppressed ROS generation and HSC senescence in irradiated mice, concordant with inhibitory effects on Wnt signaling. These findings are consistent with recent studies suggesting that Dkk1 treatment suppresses ROS generation in nonhematopoietic tissues, as well as a report demonstrating that Wnt pathway activation promotes mitochondrial ROS generation and senescence in myoblasts and fibroblasts[44,45]. However, in the hematopoietic system, several studies have suggested that activation of canonical Wnt signaling promotes HSC self-renewal[46–48]. A recent study by Lento *et al.* suggested that mice with deletion of *Ctnnb1* in hematopoietic Vav+ cells showed reduced hematopoietic progenitor cell recovery at day 14 following TBI[49]. Several factors may explain the different observations between our study and that of Lento *et al.* First, acute inhibition

of Wnt signaling with Dkk1 in the first 72 h after irradiation may have different effects on HSC regeneration as compared to that in mice with deletion of *Ctnnb1* from inception. Second, it is possible that Dkk1 mediates effects on hematopoietic regeneration via mechanisms that are independent from its inhibitory effects on canonical Wnt signaling, as observed in models of kidney epithelial repair and cardiogenesis[50,51]. As we discovered, Dkk1 acts indirectly on BM ECs, yielding a marked increase in EGF secretion, which contributed to hematopoietic regeneration. In this regard, a recent study demonstrated that ECs express LRP6, a Dkk1 receptor, and that Dkk1 and Dkk2 may regulate angiogenesis[52]. Third, the dosage of canonical Wnt pathway activation has been demonstrated to substantially impact HSCs, progenitor cells and HSC differentiation[28,53], and high dose levels of Wnt pathway activation can result in decreased HSC repopulating capacity[54,55]. Our data suggest that during the early period following radiation injury, strong induction of Wnt signaling in HSCs may be deleterious, whereas early inhibition of Wnt signaling is beneficial.

Canonical and noncanonical Wnt signaling have been shown to have discrete effects on hematopoiesis[56]. Wnt5a expression in HSCs increases with aging, causing a shift to noncanonical Wnt signaling and a decline in HSC function in older mice[57]. HSC senescence occurs over time in aged mice and is exacerbated by stress, including radiation exposure[23,37]. Here we observed that acute radiation injury increased canonical Wnt pathway activation in HSCs and that treatment with Dkk1 suppressed this signaling, in association with repression of ROS generation and HSC senescence. However, treatment with Wnt5a did not exacerbate radiation-induced ROS generation or HSC senescence. We postulate that the effects of Wnt5a and noncanonical Wnt signaling during hematopoietic aging may be distinct from the effects of noncanonical or canonical Wnt signaling in the setting of acute injury.

Over the past decade, as the cellular composition of the HSC niche has been elucidated, important questions have emerged regarding the hierarchy of cellular niche components and the manner through which niche cells communicate during their orchestration of HSC maintenance and regeneration[58,59]. Recent studies suggest that distinct BM ECs within arterial and sinusoidal blood vessels regulate HSC maintenance and activation[60]. Our results demonstrate that BM osteoprogenitors regulate hematopoietic regeneration via secretion of Dkk1, which promotes hematopoietic regeneration directly via inhibition of HSC senescence and indirectly via induction of EGF secretion by BM ECs. This latter mechanism provides a unique example of cross-talk between distinct niche cell types and highlights the importance of cooperative niche cell interactions in hematopoietic regeneration.

METHODS

Methods, including statements of data availability and any associated accession codes and references, are available in the online version of the paper.

Note: Any Supplementary Information and Source Data files are available in the online version of the paper.

1. Ding, L., Saunders, T.L., Enikolopov, G. & Morrison, S.J. Endothelial and perivascular cells maintain hematopoietic stem cells. *Nature* **481**, 457–462 (2012).
2. Ding, L. & Morrison, S.J. Hematopoietic stem cells and early lymphoid progenitors occupy distinct bone marrow niches. *Nature* **495**, 231–235 (2013).
3. Greenbaum, A. *et al.* CXCL12 in early mesenchymal progenitors is required for hematopoietic stem cell maintenance. *Nature* **495**, 227–230 (2013).
4. Méndez-Ferrer, S. *et al.* Mesenchymal and hematopoietic stem cells form a unique bone marrow niche. *Nature* **466**, 829–834 (2010).
5. Pinho, S. *et al.* PDGFR-α and CD51 mark human nestin+ sphere-forming mesenchymal stem cells capable of hematopoietic progenitor cell expansion. *J. Exp. Med.* **210**, 1351–1367 (2013).
6. Mizoguchi, T. *et al.* Osterix marks distinct waves of primitive and definitive stromal progenitors during bone marrow development. *Dev. Cell* **29**, 340–349 (2014).
7. Kunisaki, Y. *et al.* Arteriolar niches maintain hematopoietic stem cell quiescence. *Nature* **502**, 637–643 (2013).
8. Calvi, L.M. *et al.* Osteoblastic cells regulate the hematopoietic stem cell niche. *Nature* **425**, 841–846 (2003).
9. Zhang, J. *et al.* Identification of the hematopoietic stem cell niche and control of the niche size. *Nature* **425**, 836–841 (2003).
10. Visnjic, D. *et al.* Hematopoiesis is severely altered in mice with an induced osteoblast deficiency. *Blood* **103**, 3258–3264 (2004).
11. Kiel, M.J., Acar, M., Radice, G.L. & Morrison, S.J. Hematopoietic stem cells do not depend on N-cadherin to regulate their maintenance. *Cell Stem Cell* **4**, 170–179 (2009).
12. Park, D. *et al.* Endogenous bone marrow MSCs are dynamic, fate-restricted participants in bone maintenance and regeneration. *Cell Stem Cell* **10**, 259–272 (2012).
13. Maes, C. *et al.* Osteoblast precursors, but not mature osteoblasts, move into developing and fractured bones along with invading blood vessels. *Dev. Cell* **19**, 329–344 (2010).
14. Raaijmakers, M.H. *et al.* Bone progenitor dysfunction induces myelodysplasia and secondary leukemia. *Nature* **464**, 852–857 (2010).
15. Doan, P.L. *et al.* Tie2+ bone marrow endothelial cells regulate hematopoietic stem cell regeneration following radiation injury. *Stem Cells* **31**, 327–337 (2013).
16. Himburg, H.A. *et al.* Pleiotrophin regulates the retention and self-renewal of hematopoietic stem cells in the bone marrow vascular niche. *Cell Rep.* **2**, 964–975 (2012).
17. Hooper, A.T. *et al.* Engraftment and reconstitution of hematopoiesis is dependent on VEGFR2-mediated regeneration of sinusoidal endothelial cells. *Cell Stem Cell* **4**, 263–274 (2009).
18. Himburg, H.A. *et al.* Pleiotrophin regulates the expansion and regeneration of hematopoietic stem cells. *Nat. Med.* **16**, 475–482 (2010).
19. Doan, P.L. *et al.* Epidermal growth factor regulates hematopoietic regeneration after radiation injury. *Nat. Med.* **19**, 295–304 (2013).
20. Kirsch, D.G. *et al.* p53 controls radiation-induced gastrointestinal syndrome in mice independent of apoptosis. *Science* **327**, 593–596 (2010).
21. Zhang, C. *et al.* Inhibition of Wnt signaling by the osteoblast-specific transcription factor osterix. *Proc. Natl. Acad. Sci. USA* **105**, 6936–6941 (2008).
22. Rodda, S.J. & McMahon, A.P. Distinct roles for Hedgehog and canonical Wnt signaling in specification, differentiation and maintenance of osteoblast progenitors. *Development* **133**, 3231–3244 (2006).
23. Cho, J. *et al.* Purinergic P2Y receptor modulates stress-induced hematopoietic stem and progenitor cell senescence. *J. Clin. Invest.* **124**, 3159–3171 (2014).
24. Freund, A., Patil, C.K. & Campisi, J. p38 MAPK is a novel DNA damage response-independent regulator of the senescence-associated secretory phenotype. *EMBO J.* **30**, 1536–1548 (2011).
25. Chang, J. *et al.* Clearance of senescent cells by ABT263 rejuvenates aged hematopoietic stem cells in mice. *Nat. Med.* **22**, 78–83 (2016).
26. Mao, B. *et al.* Kremen proteins are dickkopf receptors that regulate Wnt–β-catenin signaling. *Nature* **417**, 664–667 (2002).
27. Boudousquié, C. *et al.* Differences in the transduction of canonical Wnt signals demarcate effector and memory CD8 T cells with distinct recall proliferation capacity. *J. Immunol.* **193**, 2784–2791 (2014).
28. Luis, T.C. *et al.* Canonical Wnt signaling regulates hematopoiesis in a dosage-dependent fashion. *Cell Stem Cell* **9**, 345–356 (2011).
29. Brault, V. *et al.* Inactivation of the β-catenin gene by *Wnt1–Cre*-mediated deletion results in dramatic brain malformation and failure of craniofacial development. *Development* **128**, 1253–1264 (2001).
30. Poulos, M.G. *et al.* Endothelial Jagged-1 is necessary for homeostatic and regenerative hematopoiesis. *Cell Rep.* **4**, 1022–1034 (2013).
31. Salter, A.B. *et al.* Endothelial progenitor cell infusion induces hematopoietic stem cell reconstitution *in vivo*. *Blood* **113**, 2104–2107 (2009).
32. Olson, T.S. *et al.* Megakaryocytes promote murine osteoblastic HSC niche expansion and stem cell engraftment after radioablative conditioning. *Blood* **121**, 5238–5249 (2013).
33. Dominici, M. *et al.* Restoration and reversible expansion of the osteoblastic hematopoietic stem cell niche after marrow radioablation. *Blood* **114**, 2333–2343 (2009).
34. Na Nakorn, T., Traver, D., Weissman, I.L. & Akashi, K. Myeloerythroid-restricted progenitors are sufficient to confer radioprotection and provide the majority of day 8 CFU-S. *J. Clin. Invest.* **109**, 1579–1585 (2002).
35. Fleming, H.E. *et al.* Wnt signaling in the niche enforces hematopoietic stem cell quiescence and is necessary to preserve self-renewal *in vivo*. *Cell Stem Cell* **2**, 274–283 (2008).
36. Varnum-Finney, B. *et al.* Notch2 governs the rate of generation of mouse long- and short-term repopulating stem cells. *J. Clin. Invest.* **121**, 1207–1216 (2011).
37. Shao, L. *et al.* Total body irradiation causes long-term mouse BM injury via induction of HSC premature senescence in an Ink4a- and Arf-independent manner. *Blood* **123**, 3105–3115 (2014).
38. Ito, K. *et al.* Regulation of oxidative stress by ATM is required for self-renewal of hematopoietic stem cells. *Nature* **431**, 997–1002 (2004).
39. Tothova, Z. *et al.* FoxOs are critical mediators of hematopoietic stem cell resistance to physiologic oxidative stress. *Cell* **128**, 325–339 (2007).
40. Taniguchi Ishikawa, E. *et al.* Connexin-43 prevents hematopoietic stem cell senescence through transfer of reactive oxygen species to bone marrow stromal cells. *Proc. Natl. Acad. Sci. USA* **109**, 9071–9076 (2012).
41. Mantel, C.R. *et al.* Enhancing hematopoietic stem cell transplantation efficacy by mitigating oxygen shock. *Cell* **161**, 1553–1565 (2015).
42. Spencer, J.A. *et al.* Direct measurement of local oxygen concentration in the bone marrow of live animals. *Nature* **508**, 269–273 (2014).
43. Luis, T.C., Ichii, M., Brugman, M.H., Kincade, P. & Staal, F.J. Wnt signaling strength regulates normal hematopoiesis, and its de-regulation is involved in leukemia development. *Leukemia* **26**, 414–421 (2012).
44. Kim, I.G. *et al.* Disturbance of DKK1 level is partly involved in survival of lung cancer cells via regulation of ROMO1 and γ-radiation sensitivity. *Biochem. Biophys. Res. Commun.* **443**, 49–55 (2014).
45. Yoon, J.C. *et al.* Wnt signaling regulates mitochondrial physiology and insulin sensitivity. *Genes Dev.* **24**, 1507–1518 (2010).
46. Huang, J. *et al.* Pivotal role for glycogen synthase kinase-3 in hematopoietic stem cell homeostasis in mice. *J. Clin. Invest.* **119**, 3519–3529 (2009).
47. Li, W. *et al.* Apc regulates the function of hematopoietic stem cells largely through β-catenin-dependent mechanisms. *Blood* **121**, 4063–4072 (2013).
48. Huang, J., Nguyen-McCarty, M., Hexner, E.O., Danet-Desnoyers, G. & Klein, P.S. Maintenance of hematopoietic stem cells through regulation of Wnt and mTOR pathways. *Nat. Med.* **18**, 1778–1785 (2012).
49. Lento, W. *et al.* Loss of β-catenin triggers oxidative stress and impairs hematopoietic regeneration. *Genes Dev.* **28**, 995–1004 (2014).
50. Lin, S.L. *et al.* Macrophage Wnt7b is critical for kidney repair and regeneration. *Proc. Natl. Acad. Sci. USA* **107**, 4194–4199 (2010).
51. Foley, A.C. & Mercola, M. Heart induction by Wnt antagonists depends on the homeodomain transcription factor Hex. *Genes Dev.* **19**, 387–396 (2005).
52. Min, J.K. *et al.* The WNT antagonist dickkopf-2 promotes angiogenesis in rodent and human endothelial cells. *J. Clin. Invest.* **121**, 1882–1893 (2011).
53. Famili, F. *et al.* High levels of canonical Wnt signaling lead to loss of stemness and increased differentiation in hematopoietic stem cells. *Stem Cell Rep.* **6**, 652–659 (2016).
54. Kirstetter, P., Anderson, K., Porse, B.T., Jacobsen, S.E. & Nerlov, C. Activation of the canonical Wnt pathway leads to loss of hematopoietic stem cell repopulation and multilineage differentiation block. *Nat. Immunol.* **7**, 1048–1056 (2006).
55. Scheller, M. *et al.* Hematopoietic stem cell and multilineage defects generated by constitutive Wnt signaling. *Nat. Immunol.* **7**, 1037–1047 (2006).
56. Malhotra, S. *et al.* Contrasting responses of lymphoid progenitors to canonical and noncanonical Wnt signals. *J. Immunol.* **181**, 3955–3964 (2008).
57. Florian, M.C. *et al.* A canonical to noncanonical Wnt signaling switch in hematopoietic stem cell aging. *Nature* **503**, 392–396 (2013).
58. Mendelson, A. & Frenette, P.S. Hematopoietic stem cell niche maintenance during homeostasis and regeneration. *Nat. Med.* **20**, 833–846 (2014).
59. Morrison, S.J. & Scadden, D.T. The bone marrow niche for hematopoietic stem cells. *Nature* **505**, 327–334 (2014).
60. Itkin, T. *et al.* Distinct bone marrow blood vessels differentially regulate hematopoiesis. *Nature* **532**, 323–328 (2016).

ONLINE METHODS

Mice. All animal procedures were performed in accordance with animal use protocols approved by UCLA and Duke University. *Osx–Cre;Bak1*^{−/−}*;Bax*^{+/−} mice were bred with *Bak1*^{−/−}*;Bax*[FL/FL] mice bearing a constitutive deletion of *Bak1* and *loxP*-flanked (floxed; FL) *Bax* alleles to generate *Osx–Cre;Bak1*^{−/−}*; Bax*[FL/−] mice and *Osx–Cre;Bak1*^{−/−}*;Bax*[FL/+] mice. *Bak1*^{−/−}*;Bax*^{+/−} and *Bak1*^{−/−}*; Bax*[FL/FL] mice were generated as previously described[15,20]. *Osx–Cre–Gfp* mice, *Ctnnb1*[FL/FL] mice, *Osx–Cherry* mice[61], and *Axin2–LacZ* mice[62] were obtained from the Jackson Laboratory (Bar Harbor, ME). *Dkk1*[FL/+] mice were generously provided by Dr. Seppo Vainio from the University of Oulu, Finland[63]. *Dkk1*[FL/+] mice were crossed with *Osx–Cre–Gfp* mice[22] to generate tissue-specific deletion of *Dkk1*. Cre-mediated recombination in *Osx–Cre–Gfp* mice is regulated by treatment with doxycycline, as both tTA and tetO are expressed under regulation of the osterix (*Sp7*) promoter (Tet-off). *Dkk1* deletion was temporally controlled in some *Osx–Cre;Dkk1*[FL/+] mice by doxycycline administration in drinking water from conception to 8 weeks of age (0.2 g doxycycline per liter water; Sigma Aldrich, St Louis, MO).

Histology and immunofluorescence staining. Hematoxylin and eosin (H&E) staining of femurs from mice was performed as previously described[15]. Femurs were fixed overnight in 4% paraformaldehyde, decalcified and paraffin-embedded. Immunofluorescence staining was performed on fixed, decalcified femurs embedded in OCT (Fisher Scientific) and sectioned with a cryostat as previously described[15]. Goat anti-osterix antibody (Santa Cruz Biotechnology, Santa Cruz, CA) was diluted 1:500 in blocking buffer (BD Biosciences) and incubated overnight at 4 °C. Slides were rinsed and incubated with Alexa Fluor 488 (AF488)-conjugated donkey anti-goat antibody (Life Technologies, Grand Island, NY) at 1:500 dilution in blocking buffer. The slides were rinsed and mounted with DAPI anti-fade Gold (Life Technologies, Carlsbad, CA). Images were obtained using an Axiovert 200 microscope (Carl Zeiss, Thornwood, NY).

Flow cytometric analysis for Osx and Dkk1. Flow cytometric analysis for osterix protein was performed on whole BM following red blood cell (RBC) lysis. Cells were stained for V450–CD45 (BD Biosciences, Franklin Lakes, NJ) and then fixed and permeabilized using the BD Cytofix–Cytoperm kit (BD Biosciences). Cells were then stained for 1 h with rabbit anti-osterix (ab94794 1:500, Abcam, Cambridge UK) and goat anti-Dkk1 (ab188597, 1:500, Abcam), rinsed and stained with AF647-conjugated anti-goat antibody (1:1,000, Life Technologies) and AF488-conjugated anti-rabbit antibody (1:1,000, Life Technologies).

Isolation of Osx⁺ bone marrow cells. Osx–Cherry mice were used to isolate Osx-labeled BM cells. BM from femurs and tibias was isolated by crushing bones and then digesting them for 10 min at 37 °C in collagenase and dispase (Sigma-Aldrich). Cells were then rinsed and depleted of lineage-committed cells with the Miltenyi lineage-depletion kit (Miltenyi Biotec, San Diego, CA). The lineage-negative fraction was stained for CD45 and sorted on a BD FACS ARIA. BM ECs were intravitally labeled by intravenous injection of 25 μg of AF647-conjugated vascular endothelial (VE)-cadherin antibody (Biolegend 138006, San Diego, CA), Biolegend, San Diego, CA) into wild-type C57BL/6 mice. Mice were euthanized 15 min after injection. CD45⁻VE-cadherin⁺ cells were identified as BM ECs and CD45⁻Osx⁺ cells were identified as Osx⁺ BM cells.

Cytokine array and enzyme-linked immunosorbent assays (ELISAs). Whole BM from one femur was collected from adult *Osx–Cre;Bak*^{−/−}*;Bax*[FL/−] mice and *Osx–Cre;Bak*^{−/−}*;Bax*[FL/+] mice at 7 d following 500 cGy TBI. After centrifugation, BM supernatants were collected into Iscove's modified Dulbecco's medium (IMDM) and analyzed for cytokine concentrations using the Quantibody mouse cytokine array C2000, according to the manufacturer's guidelines (RayBiotech, Inc., Norcross, GA). Dkk1 protein levels in the BM were confirmed by using a mouse Dkk1 ELISA kit (R&D systems, Minneapolis, MN).

Isolation and culture of BM osteoblasts and endothelial cells. To measure *Dkk1* gene and Dkk1 protein expression in BM osteolineage cells derived from *Osx–Cre;Bak*^{−/−}*;Bax*[FL/−] mice and *Osx–Cre;Bak*^{−/−}*;Bax*[FL/+] mice, BM osteolineage cells were isolated as previously described[32]. Briefly, ground bone fragments of mouse femurs and tibias were digested for 3 h with 0.2 mg/ml

collagenase, rinsed, and then plated in osteolineage cell supportive medium in 24-well plates[32]. After 3 d, bone chips were removed, and adherent colonies were observed. RNA was isolated from adherent cells for analysis of *Bax*, *Dkk1*, *Osx*, and other markers. BM endothelial cells were grown by explanting vessels flushed from the bone marrow onto 40-μm filters. Cells were grown to confluence in EGM-2 medium without EGF (Lonza, Walkersville, MD) with daily medium changes. For ELISA of PTN, EGF, and Dkk1 in the culture medium of BM osteolineage cells and BM ECs, medium was collected at day +7 of confluent cell culture. Cell culture supernatants were collected and concentrated 20-fold for ELISA analysis.

Gene expression analysis. For all studies, RNA was isolated using the Qiagen RNeasy micro kit (Qiagen, Valencia, CA). RNA was reverse-transcribed into cDNA using the iScript cDNA synthesis kit (Bio-Rad, Hercules, CA). Real-time PCR analysis for *Dkk1*, *Osx*, *Bax*, *p16*, and *Axin2* was performed using Applied Biosystems Taqman Gene Expression assays, as previously described (Life Technologies)[15]. The $2^{-\Delta\Delta CT}$ method[64] was used to quantify the change in expression of the target genes relative to that in a standard control sample. At least three technical replicates of each PCR measurement were performed. Each replicate was first normalized to the housekeeping gene *Gapdh*. Fold change relative to the control sample was then determined.

Radiation-mitigation studies. 10- to 12-week-old female C57BL/6 mice were irradiated with 800 cGy TBI, which is lethal at our institution for approximately 50% of C57BL/6 mice by day +30 (LD$_{50}$/30), using a Shepherd cesium-137 irradiator. Mice were subsequently treated with subcutaneous injections of 10 μg recombinant Dkk1 (R&D systems, Minneapolis, MN) or saline, beginning at 24 h post TBI and administered every other day through day +21. PB complete blood counts (CBC) were measured using a Hemavet 950 instrument (Drew Scientific, Miami Lakes, FL). For assessment of long-term effects of Dkk1 treatment, mice were irradiated with 600 cGy TBI and treated with the same dosage and schedule of Dkk1. At 12 weeks after TBI mice were euthanized, and hematopoietic content was analyzed. For anti-Dkk1 radiation-survival studies, 10- to 12-week-old female C57BL/6 mice were irradiated with 750 cGy TBI. Mice then received a subcutaneous injection of 100 μg goat anti-mouse-Dkk1 (AF1765, R&D Systems) or 100 μg goat IgG control (AB-108-C, R&D Systems) in a volume of 100 μl starting at 24 h after irradiation. Injections was administered every other day through day +21. To evaluate whether Dkk1 promoted survival via induction of EGF signaling, the EGF receptor inhibitor erlotinib (Sigma-Aldrich, St. Louis, MO) was administered to irradiated mice. Mice were irradiated with 500 cGy and treated subcutaneously with 10 μg Dkk1 or saline every other day, with or without 10 μg per g body weight erlotinib daily by oral gavage. Erlotinib treatment began 1 d before irradiation and continued through day +10 or +14.

Isolation of BM hematopoietic stem cells (HSCs). BM HSCs were collected from mice as previously described[18,19]. Briefly, BM cells were first treated with RBC lysis buffer (Sigma-Aldrich, St. Louis, MO), and lineage-committed cells were removed using a lineage-depletion column (Miltenyi Biotec, Auburn, CA). Lin⁻ cells were stained with allophycocyanin (APC)- and Cy7-conjugated anti-Sca-1, phycoerythrin (PE)-conjugated anti-c-kit, APC-conjugated anti-CD-34, and V450 lineage cocktail (Becton Dickinson (BD), San Jose, CA) or with isotype controls. Sterile cell sorting was conducted on a BD FACS ARIA cytometer. Purified c-kit⁺Sca-1⁺lin⁻ (KSL) and CD34⁻c-kit⁺Sca-1⁺lin⁻ (CD34⁻KSL) cells were collected into IMDM (Life Technologies) + 10% FBS + 1% penicillin–streptomycin.

CFC assays, HSC cultures, and competitive-repopulation assays. CFC assays (colony-forming unit–granulocyte monocyte (CFU-GM), burst-forming unit–erythroid (BFU-E), and colony-forming unit–mix (CFU-GEMM)) were performed as we have previously described[15,18]. For *in vitro* cultures, BM CD34⁻KSL, KSL, and lineage-negative cells were cultured in TSF medium (IMDM, 10% FBS, 1% penicillin–streptomycin, 20 ng/ml thrombopoietin (TPO), 125 ng/ml SCF, 50 ng/ml Flt-3 ligand). SCF, Flt-3 ligand, and TPO were purchased from R&D Systems. For competitive-repopulation assays, BM cells were isolated from donor 10- to 12-week-old female CD45.2⁺ mice. Recipient 10-week-old female CD45.1⁺ B6.SJL mice were irradiated with 950 cGy TBI

using a cesium-137 irradiator, and donor BM cells were then administered via tail vein injection along with a competing dose of 2×10^5 non-irradiated host BM cells. Multilineage donor hematopoietic cell engraftment was measured in the PB by flow cytometry, as previously described[15,18,19].

In vitro ROS and senescence assays. BM CD34−KSL, KSL, and lineage-negative cells were isolated by FACS and irradiated with 300 cGy. Cells were cultured in the following conditions: TSF medium, TSF + 500 ng/ml mouse Dkk1 (R&D Systems), TSF + 100 ng/ml mouse Wnt3a (R&D Systems), or TSF + 200 ng/ml mouse Wnt5a (R&D Systems). After 24 h, cells were analyzed by flow cytometry for mitochondrial ROS, active caspase-3–caspase-7, p38 phosphorylation, SA–β-gal, and intracellular glutathione (GSH). MitoSOX Red detection reagent (Life Technologies) was incubated at 5 μM in Hank's buffered saline solution (HBSS, Fisher Scientific) for 30 min at 37 °C. Cells were then rinsed and analyzed on a BD FACS CANTO-2 instrument to detect mitochondrial ROS. A Vybrant FAM Caspase-3 and Caspase-7 Assay Kit (Life Technologies) was used to detect active caspase-3 and caspase-7. Analysis of phospho-p38 was performed on cells that were fixed in 2% paraformaldehyde for 10 min and permeabilized in ice-cold methanol for 30 min. Cells were then stained with primary antibodies against phospho-p38 (50-191-935, Cell Signaling Technologies) followed by staining with appropriate secondary antibodies. SA–β-gal activity in live cells was quantified using the Enzo Life Sciences SA–β-gal kit (Enzo, Farmingdale NY). Intracellular GSH was detected using the Thiol Green intracellular GSH kit (Abcam) per the manufacturer's instructions.

Axin2–LacZ reporter analysis. Analysis of Wnt pathway activation was determined using the Axin2–LacZ reporter mouse (Jackson Laboratory), as previously described[27]. Mice were irradiated with 500 cGy and treated with or without 10 μg Dkk1 subcutaneously. At 24 h, the mice were euthanized and analyzed for LacZ signal by flow cytometry in BM CD34−KSL, KSL, and lineage-negative cells using the LacZ intracellular detection kit (Abcam). After staining for cell surface markers, cells were incubated for 1 min at 37 °C with the LacZ fluorescent substrate reagent and then placed immediately on ice before FACS analysis.

Analysis of β-catenin-deficient hematopoietic stem and progenitor cells. Loss-of-function β-catenin studies were performed by infecting KSL cells that were isolated from *Ctnnb1*[FL/FL] mice[29] with viral Cre–GFP (FCT072 LV-CMV-Cre-GFP, Kerafast, Inc., Boston, MA) or sham GFP vectors (FCT003 LV-CMV-GFP, Kerafast). BM KSL cells were isolated by FACS from *Ctnnb1*[FL/FL] mice and then plated overnight in X-Vivo 15 medium (Lonza) containing 125 ng/ml SCF, 100 ng/ml Flt-3 ligand, and 100 ng/ml TPO. After 24 h, the cells were transduced by the addition of 5 ng/ml polybrene (Fisher Scientific) and lentiviral particles for a multiplicity of infection (MOI) of 25. At 72 h, the cultures were sorted for GFP+ cells and *Ctnnb1* knockdown was confirmed by RT–PCR. The sorted cells were then irradiated with 300 cGy and placed in culture with TSF or TSF + 500 ng/ml Dkk1. For ROS studies, cultures were collected at 1 h after treatment with 300 cGy irradiation, with TSF with or without 500 ng/ml Dkk1, and analyzed as previously described. For CFCs, cultures were collected 4 d after irradiation and plated in CFC assays.

ROS scavenger assay. For ROS inhibition with *N*-acetylcysteine (NAC, Life Technologies), NAC was added to cultures at a concentration of 10 μM for 12 h before irradiation. KSL cells were irradiated with 300 cGy and then cultured for 24 h with or without 500 ng/ml Dkk1 before plating in CFC assays.

Statistical analysis. GraphPad Prism 6.0 was used for all statistical analyses. All data were checked for normal distribution and similar variance between groups. Data were derived from multiple independent experiments from distinct mice or cell culture plates. Sample sizes for *in vitro* studies were chosen based on observed effect sizes and standard errors from prior studies. For all animal studies, a power test was used to determine the sample size needed to observe a twofold difference in means between groups with 0.8 power using a two-tailed Student's *t*-test. All animal studies were performed using sex- and age-matched animals, with wild-type littermates as controls. Animal studies were performed without blinding of the investigator, and no animals were excluded from the analyses. All comparisons performed were done using a two-tailed Student's *t*-test, unless otherwise indicated in the figure legends. Values are reported as mean ± s.e.m., unless stated otherwise.

61. Strecker, S., Fu, Y., Liu, Y. & Maye, P. Generation and characterization of osterix–Cherry reporter mice. *Genesis* **51**, 246–258 (2013).
62. Lustig, B. *et al.* Negative feedback loop of Wnt signaling through upregulation of conductin (Axin2) in colorectal and liver tumors. *Mol. Cell. Biol.* **22**, 1184–1193 (2002).
63. Pietilä, I. *et al.* Secreted Wnt antagonist dickkopf-1 controls kidney papilla development coordinated by Wnt7b signaling. *Dev. Biol.* **353**, 50–60 (2011).
64. Livak, K.J. & Schmittgen, T.D. Analysis of relative gene expression data using real-time quantitative PCR and the $2^{-\Delta\Delta CT}$ method. *Methods* **25**, 402–408 (2001).

SUPPLEMENTARY INFORMATION

Supplementary Figure 1
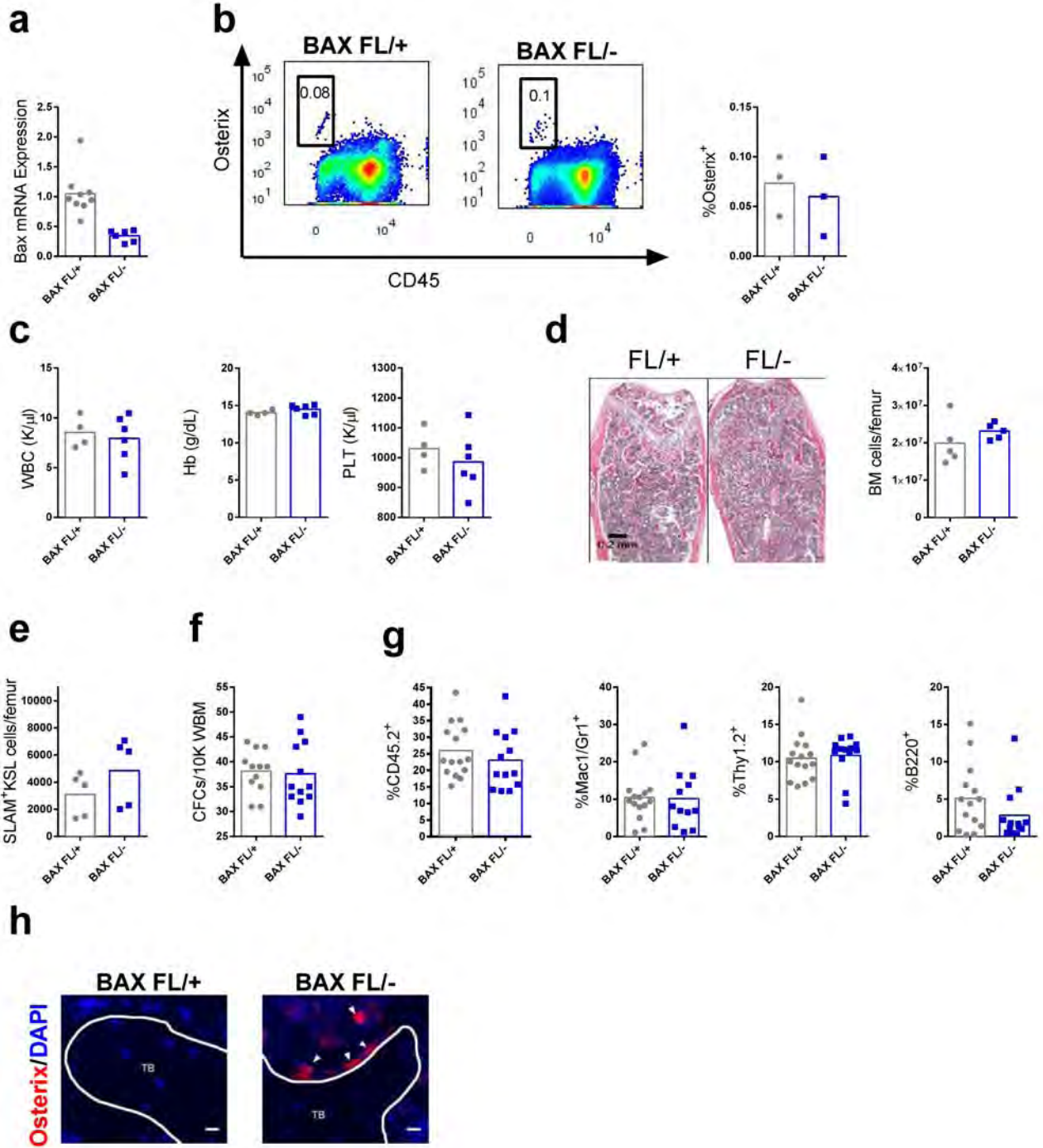
Supplementary Figure 1. Baseline hematopoietic profile of *OsxCre;Bak1*^{-/-}*;Bax*[FL/-] mice.

(a) Mean expression (±SEM) of *Bax* in *OsxCre;Bak1*^{-/-}*;Bax*[FL/+] mice (FL/+) and

OsxCre;Bak1^{-/-}*;Bax*[FL/-] mice (FL/-) *P=0.006 (FL/+, n=9 technical replicates; FL/-, n=6 technical

replicates). **(b)** Flow cytometric analysis shows the percentage of BM osterix+ cells in the CD45-

negative BM in BAX FL/+ and BAX FL/- mice at baseline. Mean %osterix+ cells are at right (n=3

mice/group). **(c)** Mean peripheral blood WBCs, hemoglobin and platelet counts in the

represented mice (FL/+, n=4 mice; FL/-, n=6 mice). **(d)** At left, H & E stained femurs from FL/+

and FL/- mice are shown (10x). At right, mean BM cell counts are shown from FL/+ and FL/-

mice at baseline (n=5 mice/group). **(e)** Mean numbers of SLAM+KSL cells (n=5 mice/group)

and **(f)** mean BM CFCs in FL/+ mice and FL/- mice (n=12 assays/group). **(g)** Mean donor

CD45.2+ cell engraftment, Mac1/Gr1 (myeloid) cell, Thy1.2+ (T cell) and B220+ (B cell)

engraftment at 12 weeks in recipient mice competitively transplanted with 1×10^5 BM cells from

FL/+ mice or FL/- mice (FL/+, n=15 mice; FL/-, n=13 mice. **(h)** Microscopic image of BM

osterix+ cells following 500 cGy TBI. At left, high power magnification view (63x) of BM osterix-

expressing cells (red) at day +3 following 500 cGy TBI in *OsxCre;Bak1*^{-/-}*;Bax*[FL/+] mice (BAX

FL/+) and *OsxCre;Bak1*^{-/-}*;Bax*[FL/-] mice (BAX FL/-). Trabecular bone (TB) is outlined in white

and white arrowheads denote osterix+ cells (scale bar 10 μm).

Supplementary Figure 2
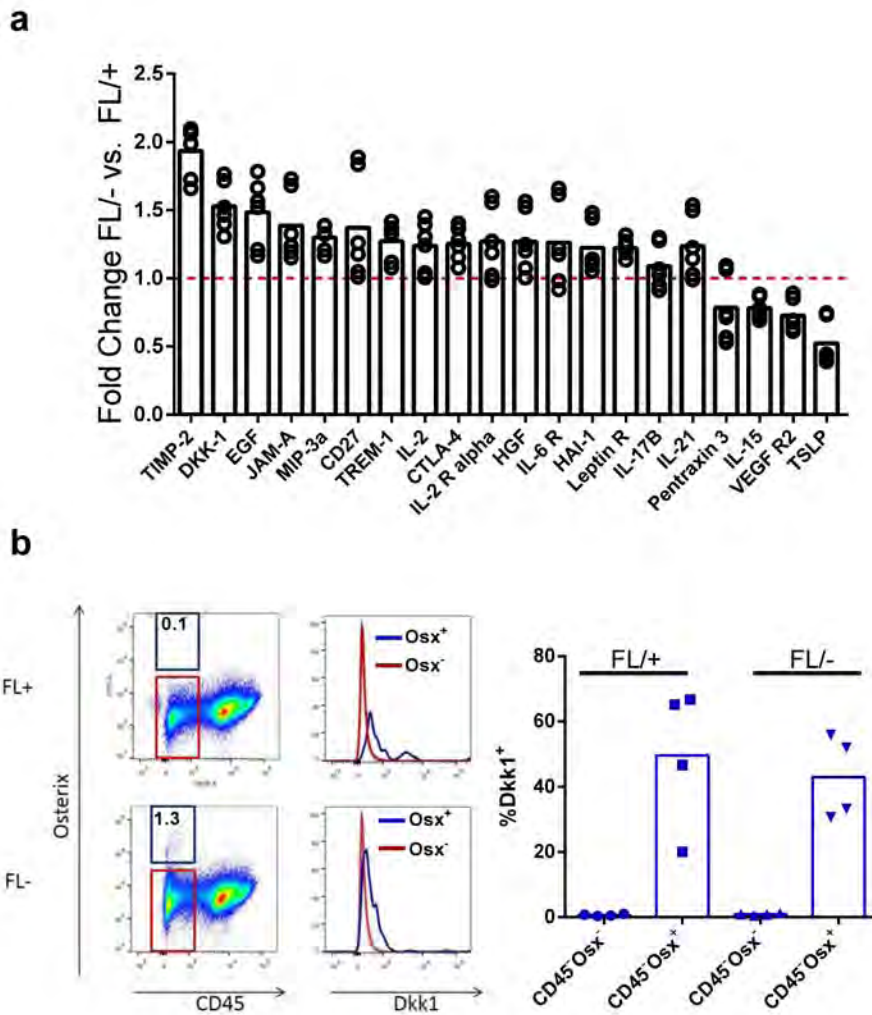
Supplementary Figure 2. Dkk1 protein expression in the BM of *OsxCre;Bak1-/-; Bax FL/-* mice and in BM osterix+ cells. **(a)** Cytokine array measurement of the concentrations of upregulated (filled bars) and downregulated cytokines (open bars) in the BM of BAX FL/- and BAX FL/+ mice at day +7 following 500 cGy TBI (*n*=6 mice/group). **(b)** Flow cytometric analysis shows the percentage of Dkk1+ cells in BM osterix+ and osterix- cells within the CD45-negative BM in BAX FL/+ and BAX FL/- mice at day +3 following 500 cGy TBI. Mean %Dkk1+ cells within each population are shown at right (*n*=4 mice/group).

Supplementary Figure 3
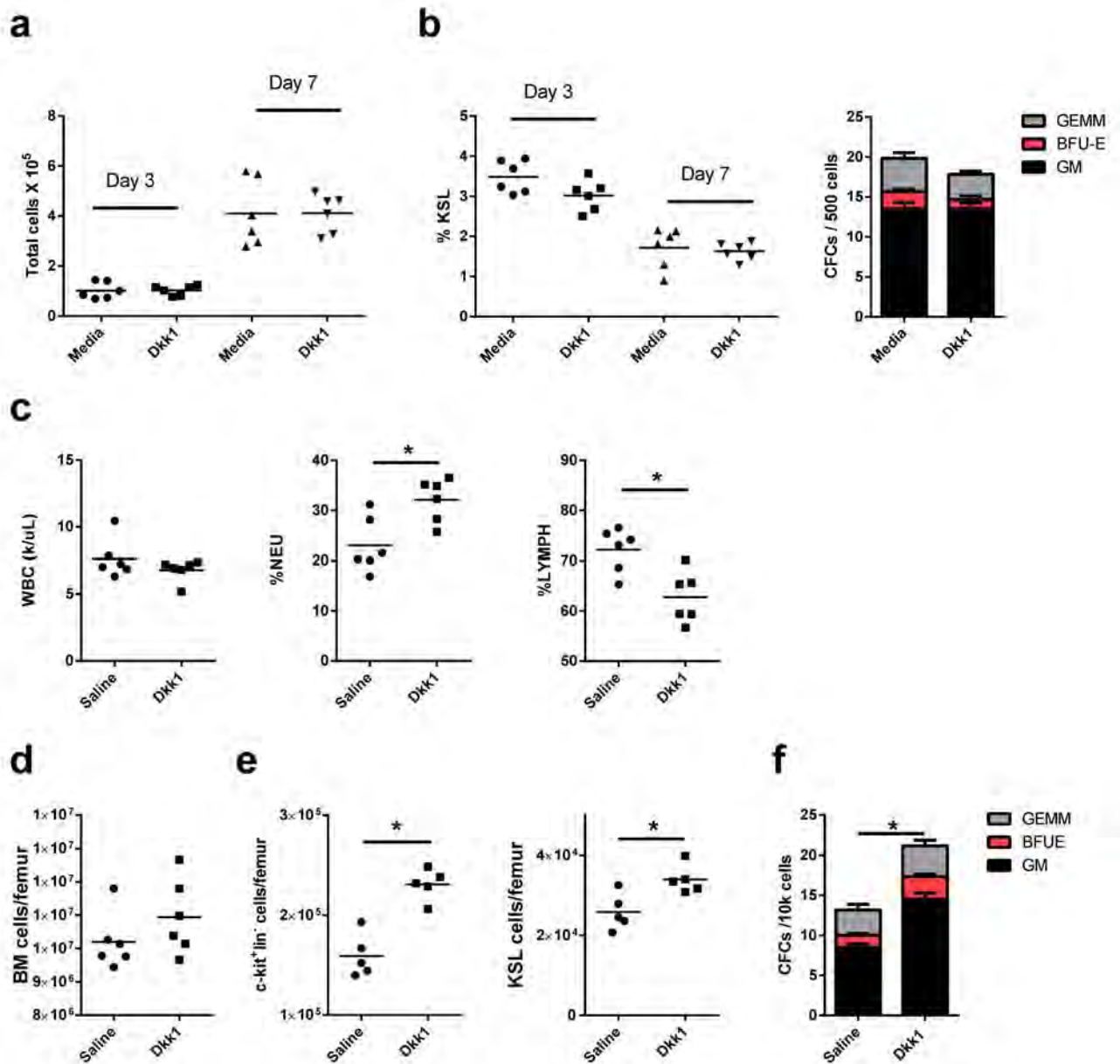
Supplementary Figure 3. Dkk1 effects on HSCs in vitro and the hematopoietic system in vivo during homeostasis. **(a)** Mean total cell numbers after 7 days of culture of non-irradiated BM KSL cells treated with cytokine media (thrombopoietin 20 ng/mL, SCF 125 ng/mL, Flt-3 ligand 50 ng/mL) with and without Dkk1 (*n*=6 replicates/group). **(b)** At left, mean percentages of KSL

cells after culture. At right, mean numbers of CFCs after culture (n=6 assays/group). **(c)** Scatter

plots of peripheral blood total WBCs, %neutrophils and %lymphocytes after 4 weeks of systemic

treatment with 10 µg Dkk1 in non-irradiated mice. *P=0.009 and *P=0.006 (n=6 mice/group).

(d) Mean BM cell counts are shown at 4 weeks in non-irradiated Dkk1 - treated mice. (n=6

mice/group). **(e)** At left, mean BM c-kit$^+$lin$^-$ cells in saline - treated and Dkk1 - treated mice. At

right, mean BM KSL cells. *P=0.001 and *P=0.01 (n=5 mice/group). **(f)** Mean numbers of BM

CFCs from non-irradiated saline-treated and Dkk1-treated mice. *P=0.0001 (n=6 assays/group).

Supplementary Figure 4
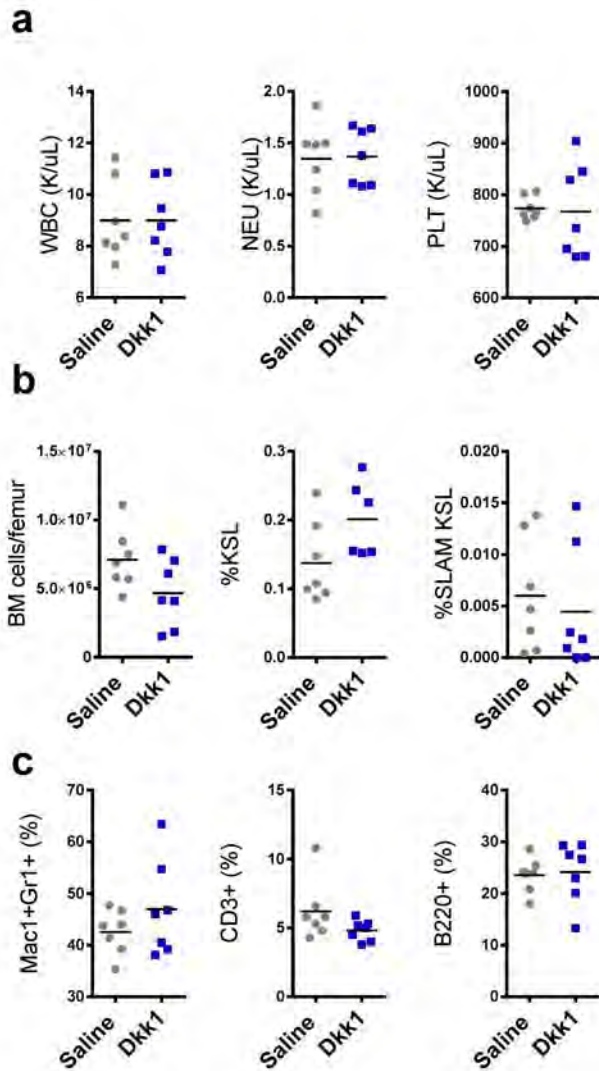
Supplementary Figure 4. Long term effects of Dkk1 treatment after radiation exposure.

(a) Analysis of mice at 12 weeks following 600 cGy TBI and treated with 10 µg Dkk1 or saline every other day x 21 days. Peripheral blood WBCs, neutrophils and lymphocytes are shown at 12 weeks (*n*=7 mice/group). **(b)** BM cell counts, %BM KSL cells and %SLAM⁺KSL cells at 12 weeks (*n*=7 mice/group). **(c)** %BM myeloid, T and B cells at 12 weeks (*n*=7 mice/group).

Supplementary Figure 5
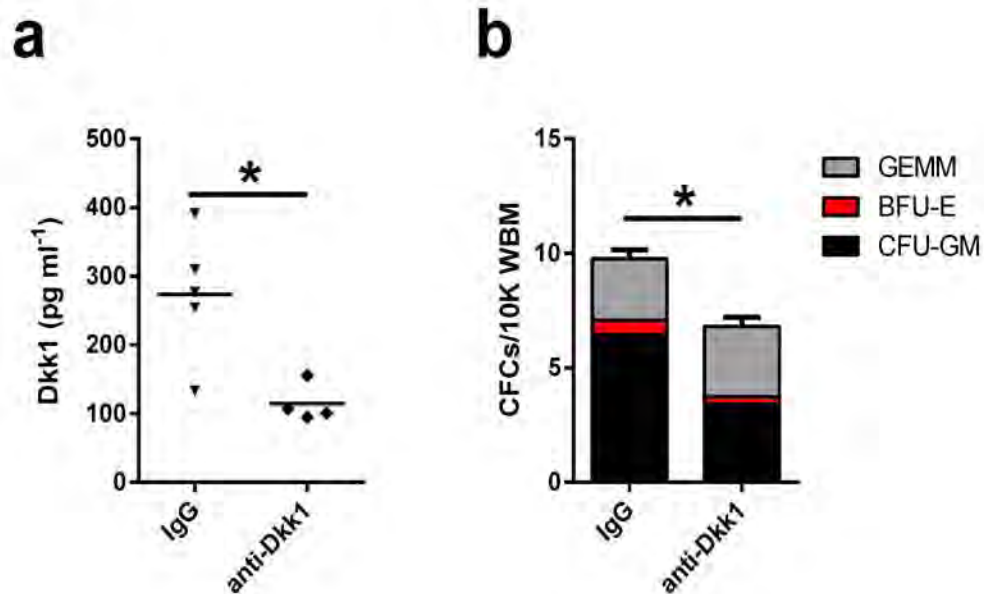
Supplementary Figure 5. Inhibition of Dkk1 suppresses hematopoietic regeneration following irradiation. **(a)** Mean Dkk1 protein levels by ELISA of the BM supernatants of mice treated with anti-Dkk1 or IgG at 24 hours after 500 cGy TBI. *P=0.01 (IgG, n=5 mice; anti-Dkk1, n=4 mice). **(b)** BM CFCs at day +10 after treatment with anti-Dkk1 or IgG. *P=0.01 (IgG, n=13 assays; anti-Dkk1, n=15 assays).

Supplementary Figure 6
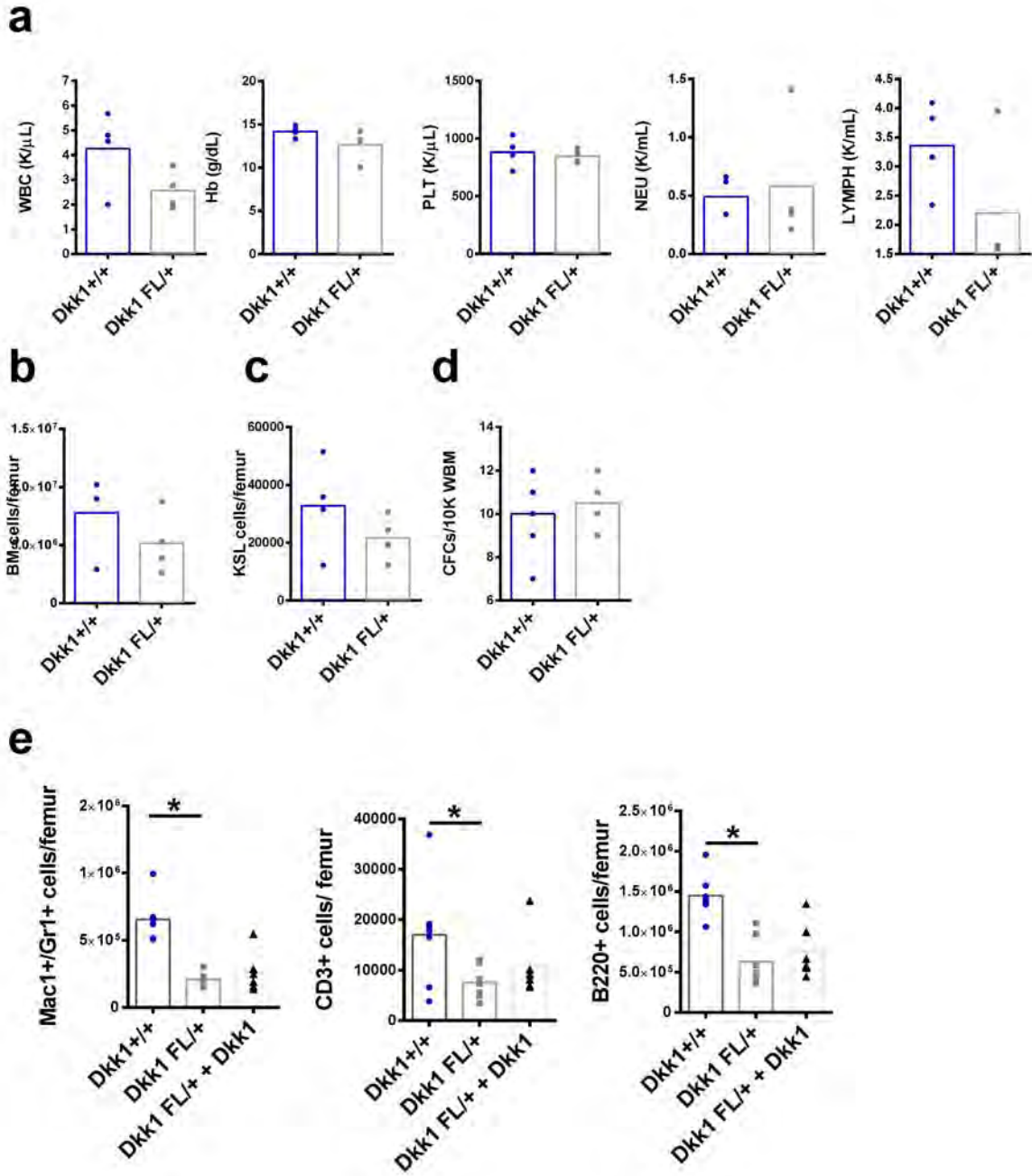
Supplementary Figure 6. Baseline hematopoietic profile of *OsxCre;Dkk1*^{FL/+} mice.

(a) Mean peripheral blood complete blood counts are shown in 8 week old *OsxCre;Dkk1*^{FL/+} mice (Dkk1 FL/+) and *Dkk1*^{+/+} mice (Dkk1 +/+)(n=4 mice/group). **(b)** BM cell counts, **(c)** KSL counts and **(d)** CFCs are shown for each group (n=4 mice/group). **(e)** Dkk1 FL/+ mice and Dkk1+/+ mice were irradiated with 500 cGy TBI and an additional group of Dkk1 FL/+ mice were treated with 10 µg Dkk1 every other day through day +10. Mean numbers of BM myeloid, T and B cells at day +10. *P=0.01 for myeloid; *P=0.03 for T cells; *P<0.001 for B cells (Dkk1+/+, n=7 mice; Dkk1 FL/+, n=7 mice; Dkk1 FL/+ + Dkk1, n=6 mice).

Supplementary Figure 7
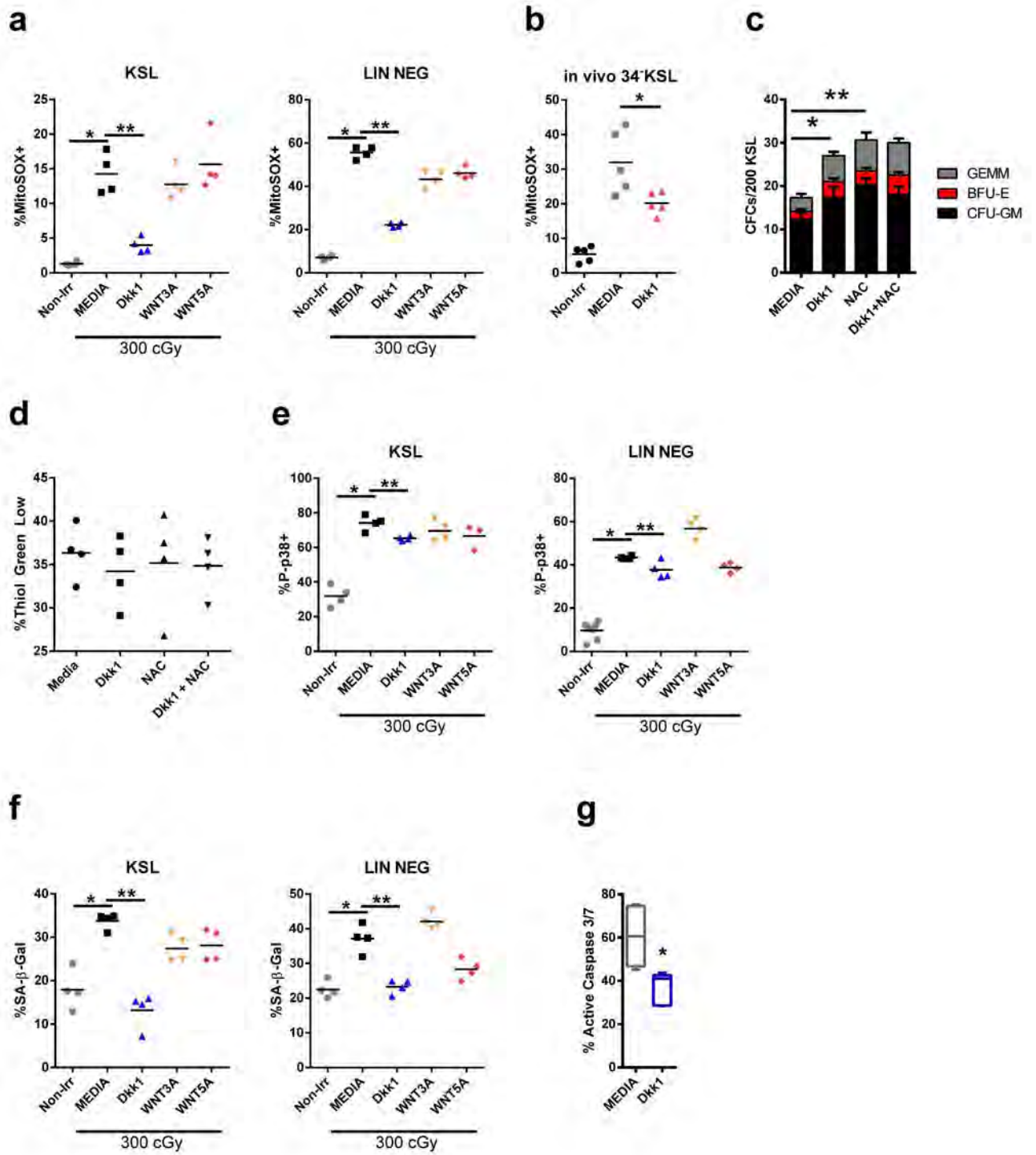
Supplementary Figure 7. Dkk1 suppresses mitochondrial ROS generation, P38 activation, and senescence in hematopoietic progenitor cells following irradiation. **(a)** At left, scatter plots of mitochondrial ROS levels in KSL cells and lineage negative cells at 24 hours following 300 cGy and treatment with or without 500 ng/mL Dkk1. KSL cells, *P=0.0001, **P=0.0006; Lin⁻ cells, *P< 0.0001, **P< 0.0001 (n=4 replicates/group). **(b)** In vivo mitochondrial ROS levels in KSL cells at 24 hours after 500 cGy TBI and treatment with 10 µg Dkk1 or saline. *P= 0.03 (n=5 mice/group). **(c)** Mean numbers of CFCs recovered from irradiated BM KSL cells at day +2 of treatment with TSF ± Dkk1 ± N-acetylcysteine (NAC). *P<0.001, **P<0.001 (n=6 assays/group). **(d)** GSH levels measured by Thiol Green⁺ cells in BM KSL cells at 24 hours after 300 cGy and treatment with 10 µM NAC (n=4 cultures/group). **(e)** Phospho-p38 levels in BM KSL cells and Lin⁻ cells at 24 hours following 300 cGy and treatment with or without 500 ng/mL Dkk1. KSL cells, *P=0.0001, **P=0.008; Lin⁻ cells, *P< 0.0001, **P< 0.03 (n=4 cultures/group). **(f)** SA-β-gal levels in irradiated BM KSL and Lin⁻ cells at 24 hours of culture with or without 500 ng/mL Dkk1. KSL cells, *P=0.0007, **P<0.0001; Lin⁻ cells, *P=0.0008, **P=0.0008 (n=4 cultures/group). **(g)** Whisker plots showing percentage of BM KSL cells with Caspase 3/7 activation at 1 hour following 300 cGy and treatment with or without 500 ng/mL Dkk1. *P=0.006 (n=6 cultures/group).

Supplementary Figure 8
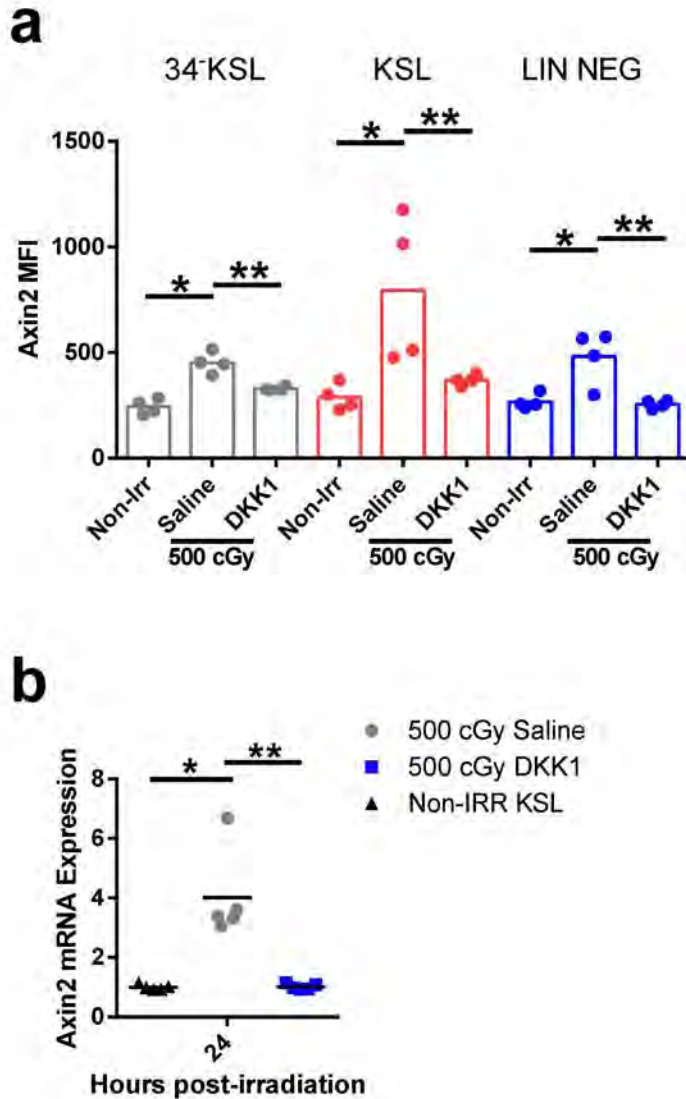
Supplementary Figure 8. Dkk1 suppresses Wnt pathway activation in irradiated hematopoietic stem and progenitor cells. **(a)** Mean fluorescence intensity (MFI) of LacZ in BM CD34⁻KSL, KSL, and lin⁻ cells at 24 hours after 500 cGy TBI and treatment with 10 µg Dkk1. 34⁻KSL cells, *P=0.0009, **P=0.003; KSL cells, *P=0.03, **P=0.03 (Mann-Whitney test); Lin⁻ cells, *P=0.01,

P=0.01 (*n*=4 mice/group). **(b) RT-PCR analysis of Axin2 gene expression in KSL cells from

C57Bl6 mice at 24 hours after 500 cGy TBI and treatment with or without 10 µg Dkk1. *P=0.002,

**P= 0.002 (*n*=5 mice/group).

Supplementary Figure 9
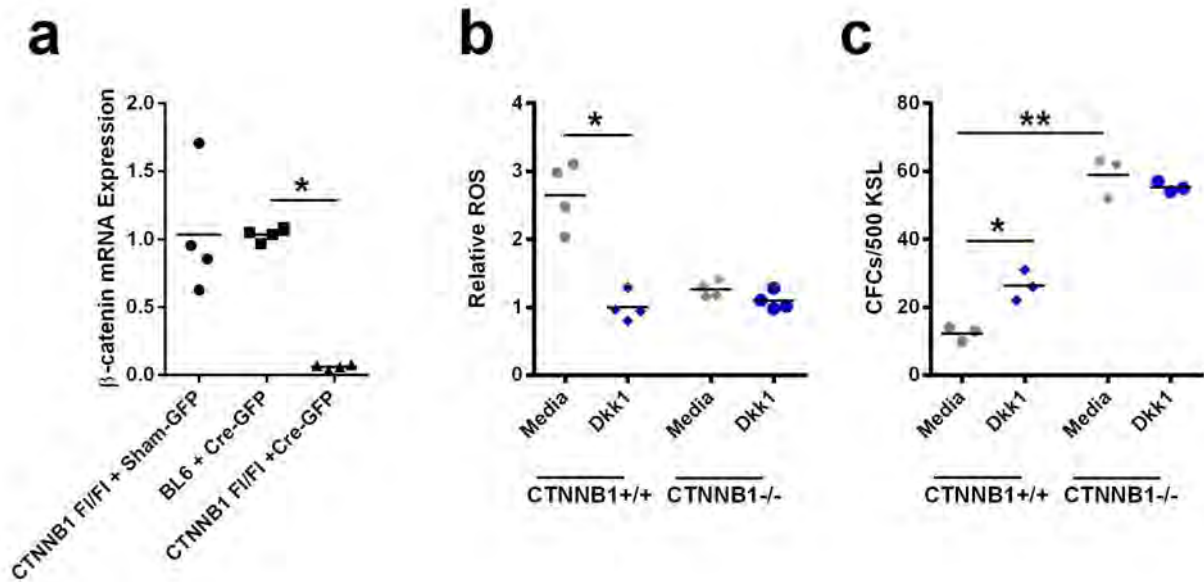
Supplementary Figure 9. Dkk1 suppresses Wnt Signaling in HSCs following irradiation.

(a) Mean β-catenin expression levels after viral Cre-mediated deletion of *CTNNB1* in BM KSL cells from *CTNNB1* FL/FL and wild-type controls. *P<0.0001 (n=4 cultures/group). **(b)** Scatter plots of ROS levels at 1 hour following 300 cGy and treatment of *CTNNB1*^{+/+} and *CTNNB1*^{-/-} BM KSL cells with or without 500 ng/mL Dkk1. *P=0.01 (*n*=4 cultures/group). **(c)** Scatter plots of CFCs from irradiated *CTNNB1*^{+/+} and *CTNNB1*^{-/-} BM KSL cells at day +4 following treatment with or without 500 ng/mL Dkk1. *P=0.008, **P=0.002 (*n*=3 assays/group).

Supplementary Figure 10
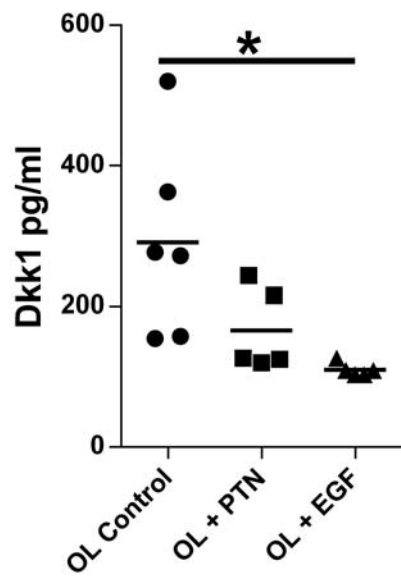
Supplementary Figure 10. Dkk1 protein secretion is suppressed by EGF treatment.

Dkk1 levels in the culture media of primary BM osteolineage cells (OL) at day +7 following

treatment with 100 ng/mL PTN or 20 ng/mL EGF. *P=0.02 (n=5 cultures/group).